

MINERALOGY OF TAILINGS FROM THE MOUNT NANSEN SITE, YUKON

Prepared for: **Energy Mines and Resources,
Yukon Government**
Whitehorse, Yukon

November 2005



J.L. Jambor
Leslie Investments Ltd
Research and Consulting
316 Rosehill Wynd
Tsawwassen, B.C. V4M 3L9
Ph: (604) 948-1368
E-mail: JLJambor@aol.com

EXECUTIVE SUMMARY

Six samples of tailings from the former Mount Nansen mine, Yukon, were mineralogically examined primarily to determine whether mineral species susceptible to destabilization under reducing conditions are present. The principal candidates that would be amenable to such reductive effects in the tailings setting are ferric iron oxyhydroxides, which are well-known sorbers of heavy metals and semi-metals such as Cu, Zn, and As.

All six of the tailings samples are quartz-rich, and five of the samples also contain major amounts of carbonate minerals. Pyrite [FeS₂] is by far the predominant sulfide mineral and locally occurs in percentage amounts. Arsenopyrite [FeAsS] and sphalerite [(Zn,Fe)S] are present in small amounts in all samples and are the principal primary sources of As and Zn, respectively. Chalcopyrite [CuFeS₂] and galena [PbS] occur locally in minute amounts and are the main primary sources of Cu and Pb, respectively.

The principal secondary phase is Fe oxyhydroxide; other secondary minerals detected to occur at least locally include gypsum [CaSO₄·2H₂O], jarosite [KFe₃(SO₄)₂(OH)₆], plumbojarosite [PbFe₆(SO₄)₄(OH)₁₂], covellite [CuS], and Fe arsenate that forms oxidation rims on arsenopyrite. Although the Fe oxyhydroxides have been observed in all samples, they are most abundant in the beach and shallow-water tailings. Numerous microbeam analyses indicate that the Fe oxyhydroxides are highly variable in composition, but Cu, Zn, and As are commonly detectable in their energy-dispersion spectra. Large particles of Fe oxyhydroxide are especially abundant in the tailings sample from the north beach. The oxyhydroxide from this site is typically highly heterogeneous on a micrometres scale and likely contains a Ca-dominant carbonate phase as well as appreciable amounts of non-sulfide Cu. Reductive dissolution of the ferric Fe oxyhydroxides and other secondary minerals would result in the release of Cu, Zn, Pb, and As.

CONTENTS

INTRODUCTION	3
SAMPLES AND METHODS	3
RESULTS	4
<i>Sample 004A</i>	5
<i>Sample 004B</i>	13
<i>Sample 005</i>	20
<i>Sample 006</i>	28
<i>Sample 007</i>	38
<i>Sample 008</i>	41
<i>Sample 009</i>	45
CONCLUSIONS	46
APPENDIX	54

INTRODUCTION

The Mount Nansen former Au–Ag mine is about 60 km west of Carmacks, Yukon. Modest tonnages (<1 Mt) of ore were milled on-site during highly sporadic production from 1968 to 1999. The site was abandoned by private interests in 1999 and is currently under government maintenance. Part of the ongoing rehabilitation program presumably involves revegetation, and Lorax Environmental Services has expressed a concern that fertilization may lead to increased algal growth in the tailings-storage facility; the increased organic content in turn may result in the development of reducing conditions at the tailings – water interface. Previous observations at other tailings sites have indicated that remobilization of sorbed trace elements such as As and Cu have occurred in the reduced conditions that followed fertilization. Therefore, the objective of the mineralogical study reported here was “to identify any problematic phases which may become destabilized under more reducing sedimentary conditions” (written communication, Lorax Environmental Services, Sept. 15, 2005).

SAMPLES AND METHODS

Six samples of Mount Nansen tailings in plastic bags were received by LRC on September 21, 2005. Data for the collection sites are given in Table 1. None of the samples was dry, and some consisted of a mixture of solids and free-flowing aqueous fluid. All of the samples were removed from their bags and were placed in, or on, plastic receptacles, and were allowed to dry at room temperature. The drying process took almost a week to complete because of the large amount of fluid in some of the samples. Monitoring during the drying period did not reveal colour changes attributable to further oxidation, and only on sample 004 was a minute amount of

Table 1. Collection sites of the tailings samples

Sample	GIS Lat	Long	Depth, m
004	62°02.534'	137°07.066'	beach, North end
005	62°02.527'	137°07.034'	0.84
006	62°02.527'	137°07.061'	0.3
007	62°02.509'	137°06.951'	1.68
008	62°02.531'	137°06.939'	2.13
009	62°02.536'	137°06.852'	beach, South end

surficial precipitate observed to have formed. The precipitate occurred as a peppering of sub-millimeter white to colourless blebs; a small intact piece of bleb-bearing sample was removed for subsequent further examination.

Each of the dried samples was only weakly cemented and could be pulverized using only forefinger pressure. However, the finest grained samples (004, 007, and 008) required more finger pressure than samples 009 and an apparently coarser fraction within 004. Sample 004 was therefore crudely split into a coarse fraction (004B) and the remnant bulk sample (004A); the 004B sample was obtained simply by hand-picking of some of the coarser grained pieces.

Each of the samples was hand-pulverized as indicated above, and was split to yield a sample for mineralogical examination. Each of the mineralogical samples was further split, with one portion submitted to Vancouver Petrographics for the preparation of optical sections, and the other retained for possible X-ray diffractometry. The optical sections were prepared as polished thin-sections on 26 × 46 mm glass slides. To minimize the dissolution of possible water-soluble minerals, it was specified by LRC that no water be used during section preparation.

The optical sections were received on October 31, 2005, and were examined in both transmitted and reflected light. Areas deemed to merit further study by microbeam methods were marked on the sections, and a photomicrograph was taken to aid in locating the relevant grains within each marked area. Scanning electron microscopy and energy-dispersion spectroscopic analyses (SEM-EDS) were done at 20 kV with a Philips XL-30 instrument and a coupled Princeton Gamma Tech IMIX-4 analyzer, at the Department of Earth and Ocean Sciences, University of British Columbia (UBC). X-ray diffractometry was done with a Siemens rotating-anode instrument at UBC; details of the Rietveld refinements that were done to obtain the quantitative mineralogy of two of the samples are given in Appendix 1.

RESULTS

Megascopic comparison of the pulverulent mineralogical samples revealed that there is little colour variation among the group. All have a slightly brownish or tan tint rather than being neutral grey; within this limited variation, sample 004B is the most ochreous, and samples 007 and 008 can be described as the lightest in colour and the least discolored.

Sample 004A

The as-received 004 material consisted of damp solids unaccompanied by a liquid phase. Although the sample was megascopically appraised to contain some of the coarsest grains in the six-sample suite, a portion of the sample consists of fine-grained, clay-size material that presumably occurred as a layer or layers in the cored interval. The overall appearance is brownish ochreous, with the clay-like material slightly lighter.

The optical section is megascopically light brown, but a few large particles or aggregates are distinctly reddish brown. No sulfides are visible.

The section viewed microscopically in transmitted light is extremely fine-grained, with maximum particle sizes only about 60 μm across. The non-opaque assemblage is quartz- and carbonate-dominant; an acid (25% HCl) test of the non-mounted fraction gave an instantaneous vigorous effervescence, indicating the presence of abundant calcite [CaCO_3] or dolomite [$\text{CaMg}(\text{CO}_3)_2$]. Otherwise, only small amounts of mica (muscovite and biotite) were readily identifiable optically, but X-ray diffractometry was performed on companion sample 004B to obtain a better resolution of the fine-grained matrix minerals and the total mineral assemblage. The megascopic distinctly reddish brown particles are fragments of Fe oxyhydroxide that are highly heterogeneous because of intergrowths and occluded tailings particles.

Although sulfides were not observed megascopically, their apparent absence arises solely because of the small size of the grains. One grain of pyrite in the section is 65 μm across; otherwise, however, the largest grains are only ~ 30 μm across, and most are < 15 μm . Only one grain of pyrite was observed to have a rim of secondary Fe oxyhydroxide. Despite its fine grain size, pyrite is relatively abundant insofar as an order-of-magnitude estimation of its content is $\sim 1\%$. Only a trace amount of galena [PbS], and possibly sphalerite [$(\text{Zn},\text{Fe})\text{S}$], was observed.

Several of the oxyhydroxide fragments were examined by EDS analysis because Fe oxyhydroxides are known well to be scavengers of trace elements, including those of the heavy metals and semi-metals. A large particle of sulfide-free Fe oxyhydroxide is shown in Figure 1, and two EDS spectra of different spots on the particle are given in Figure 2. Both spectra show that, in addition to the expected high content of Fe, the particle is rich in Ca. The relatively low Si and S contents indicate that the Ca is not attributable to the presence of a Ca silicate or a Ca sulfate (such as gypsum, $\text{CaSO}_4 \cdot 2\text{H}_2\text{O}$); thus, it is likely that the Ca occurs as calcite, or was derived from an additive such as lime [CaO] or its reaction product, portlandite [$\text{Ca}(\text{OH})_2$].

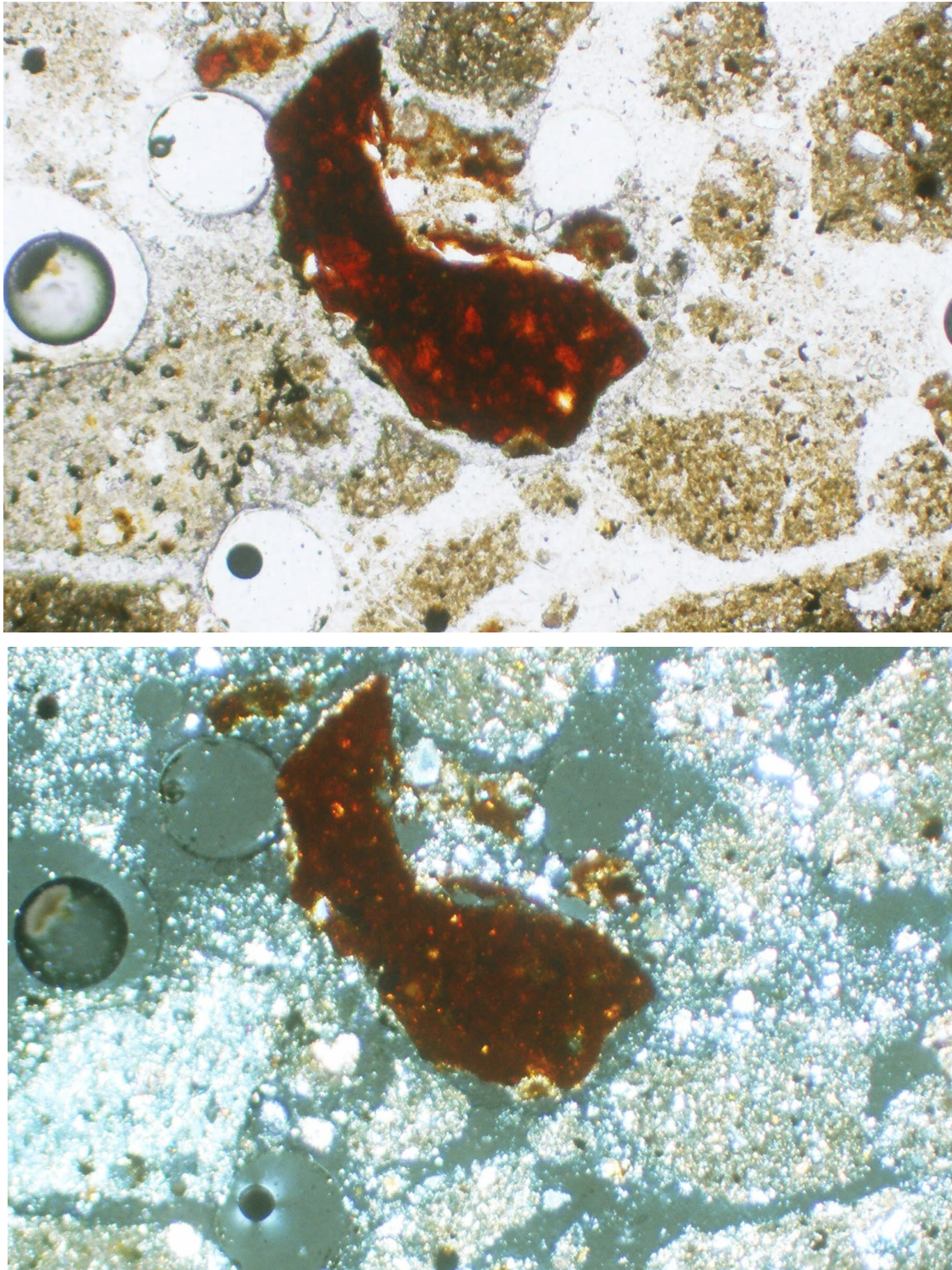


Figure 1. Sample 004A in plain transmitted light (top) and the same field with reflected light, polarizers almost crossed and internal reflection (bottom), width of field 1.3 mm, showing a large particle of heterogeneous, reddish Fe oxyhydroxide for which EDS spectra are given in Figure 2. The lower photo shows the fine-grained character of the sample, which consists predominantly of quartz.

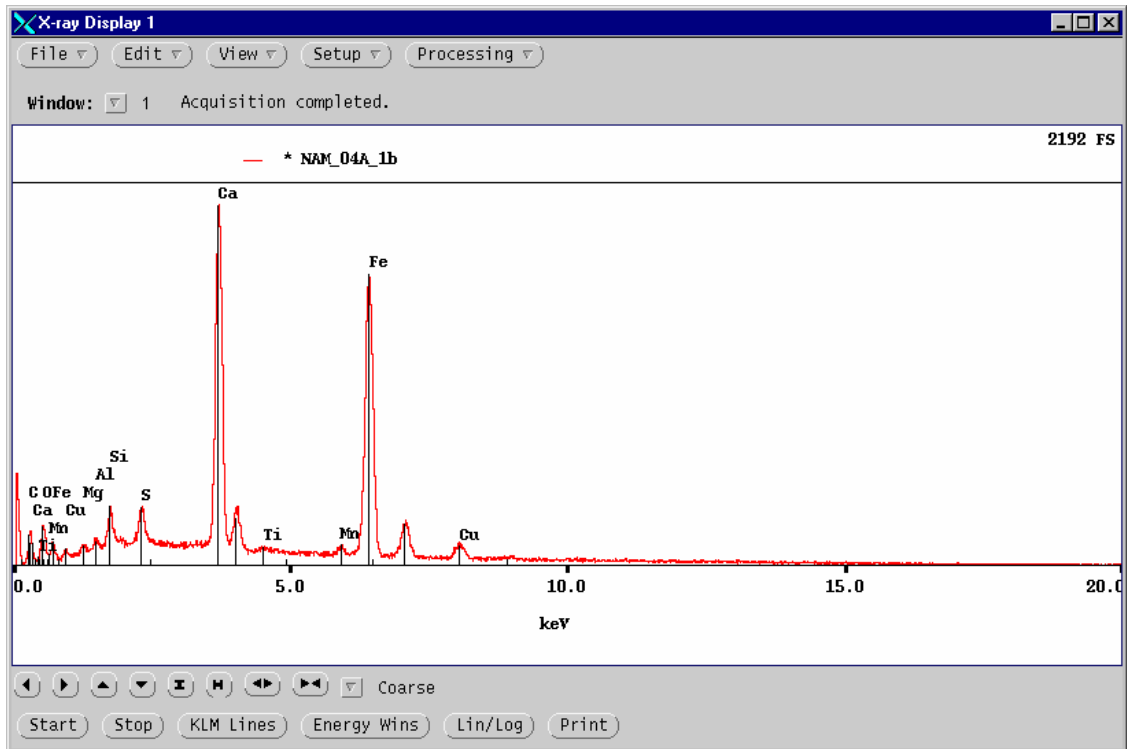
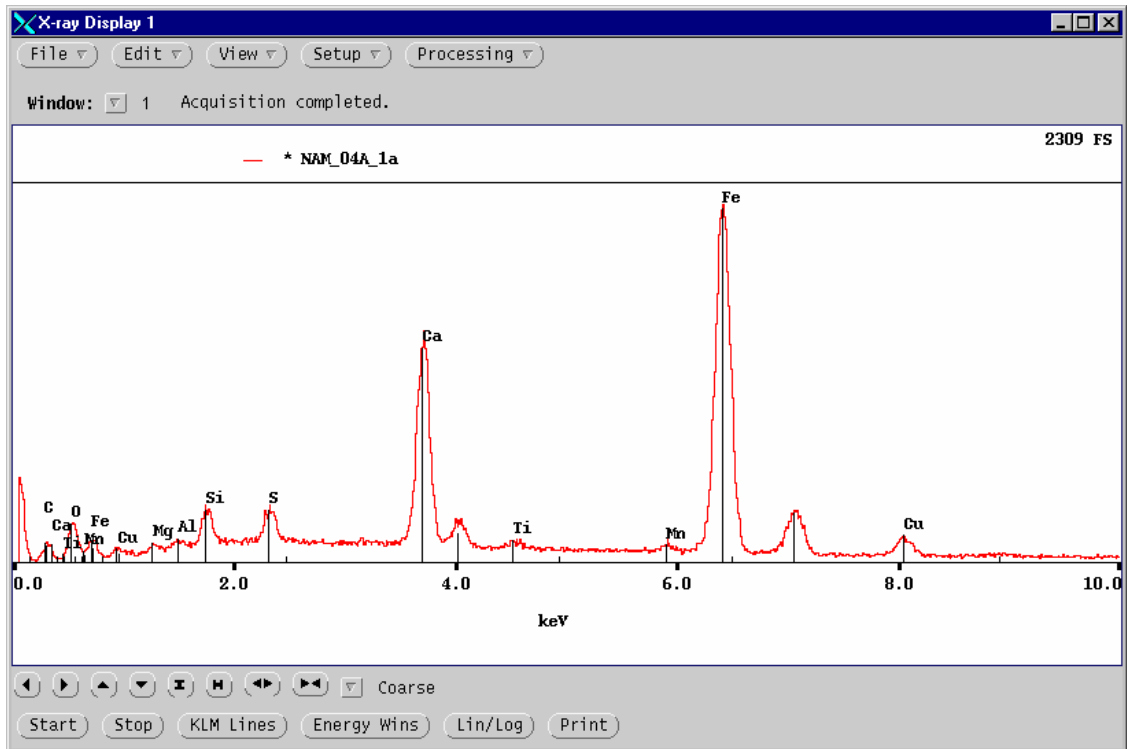


Figure 2. EDS spectra of different spots on the Fe oxyhydroxide of Figure 1. The high Ca content is a reflection of the heterogeneity of the particle.

The X-ray data for sample 004B indicate that calcite is abundant whereas the other minerals are not detectable. A significant feature of the two spectra is that, from an environmental perspective, Cu is present in relatively large amounts.

Several other particles of Fe oxyhydroxide in different areas of the section were similarly examined. Figure 3 illustrates a well-defined oxyhydroxide particle whose spectrum is not shown but is similar to those in Figure 2. Figure 4 shows two Fe-rich areas and Figure 5 gives the corresponding EDS spectra. Likewise, Figures 6 and 7 show two oxyhydroxide particles and their respective spectra. All of the oxyhydroxide particles show a consistent presence of Cu. Trace amounts of Zn erratically accompany the Cu (Figs. 5, 7), and one particle contains detectable As (Fig. 7).



Figure 3. Sample 004A in plain reflected light, width of field 0.625 mm, showing at the arrow a large particle of Fe oxyhydroxide (the circular objects are bubbles in the section). Most of the fine-grained, grey grains with moderate reflectance are quartz, but on the extreme right at mid-height is a white grain of pyrite. Despite the apparently greater homogeneity of the Fe oxyhydroxide relative to that in Figure 1, EDS spectra gave a high Ca content like that in Figure 2.

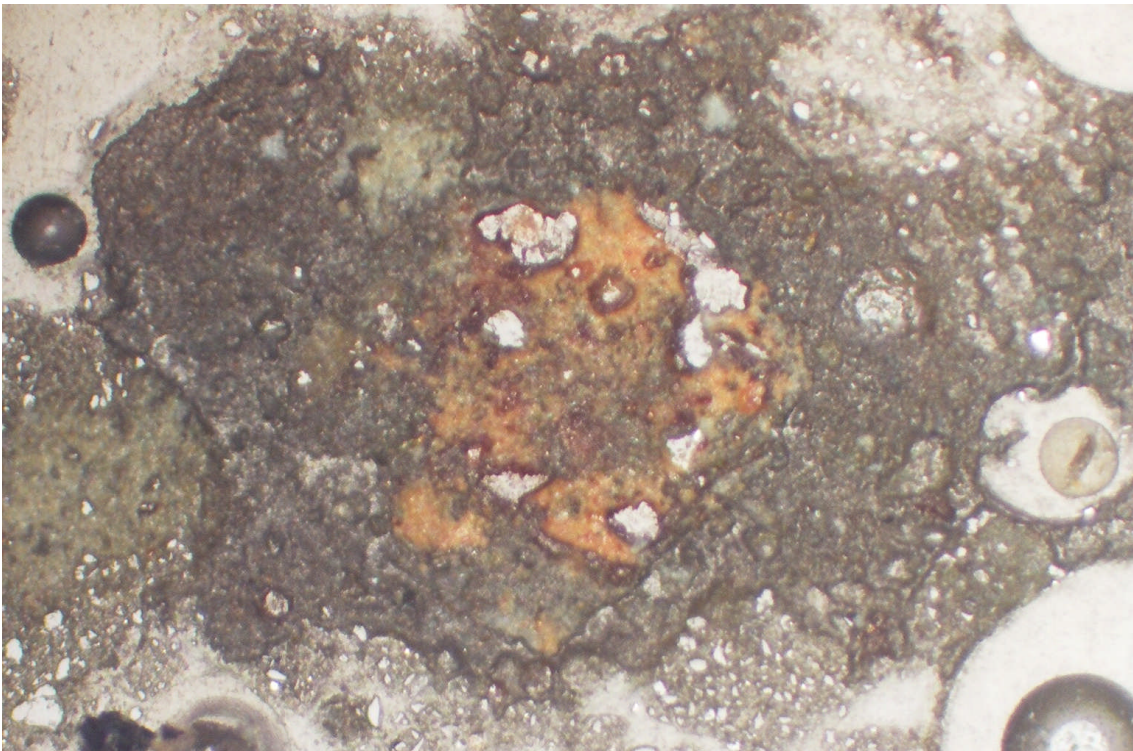
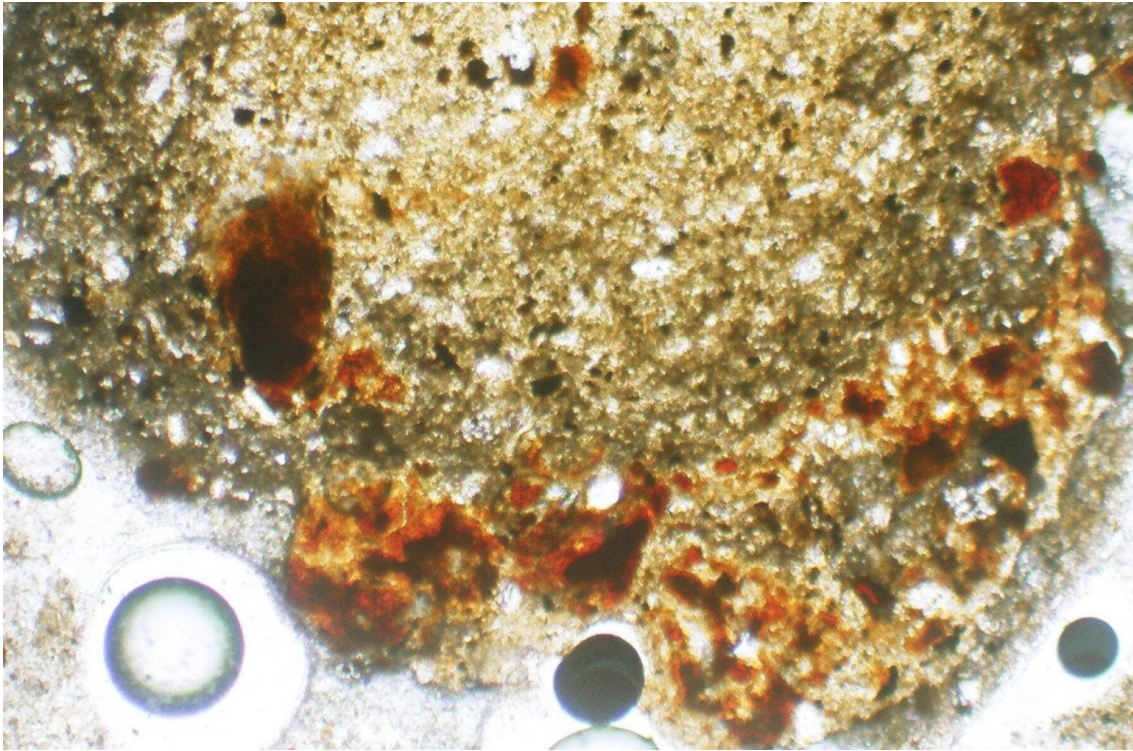


Figure 4. Sample 004A in plain transmitted light (top) and another area in plain reflected light (bottom), width of field 1.3 mm. The EDS spectra for the reddish Fe oxyhydroxide in the upper photo and in the lower photo are at the top and bottom, respectively, of Figure 5.

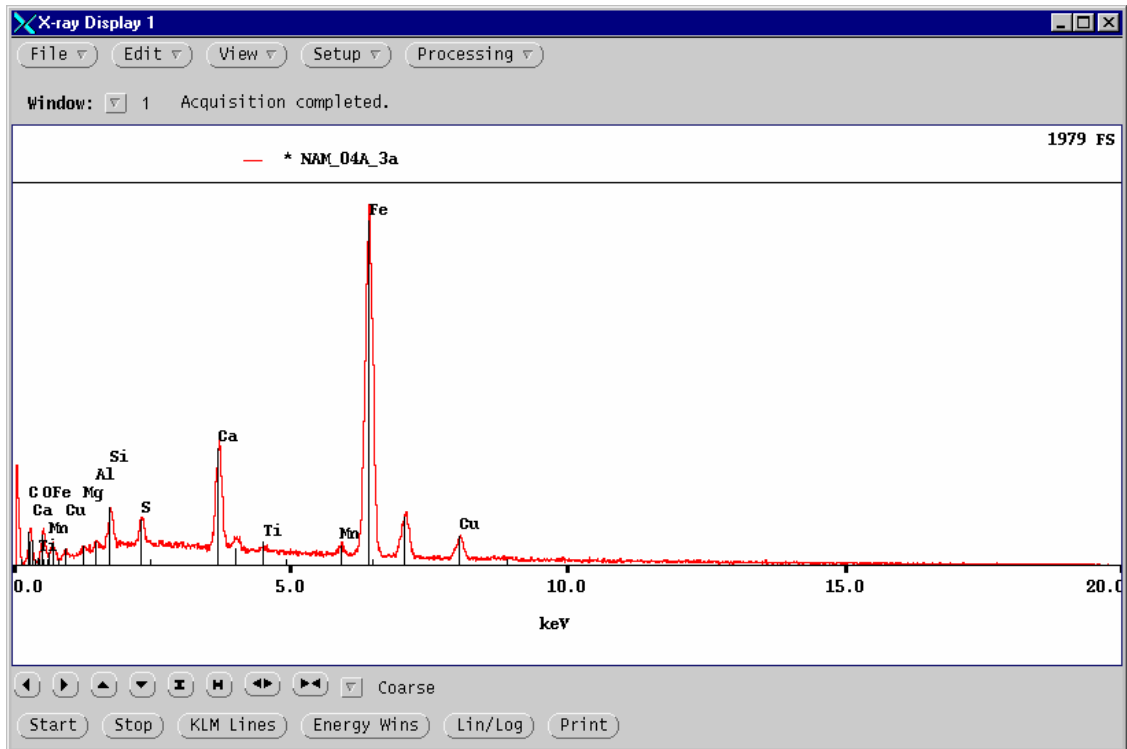
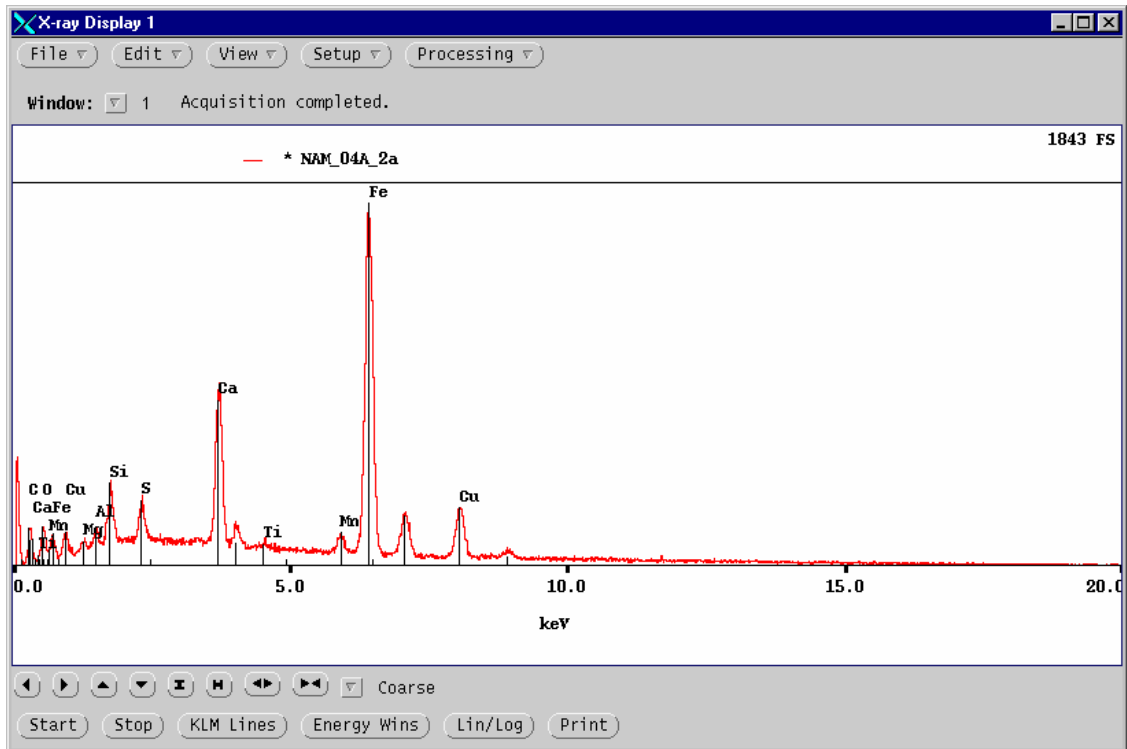


Figure 5. EDS spectra for the Fe-oxyhydroxide particles in Figure 4. The upper spectrum is for the large particle at mid-height on the left in the upper photo of Figure 4, but similar spectra were obtained from the adjacent particles. The bottom spectrum is for the large oxyhydroxide particle at the centre of the lower photo of Figure 4. The small unlabelled peak to the right of the Cu peak in the upper spectrum is for Zn.

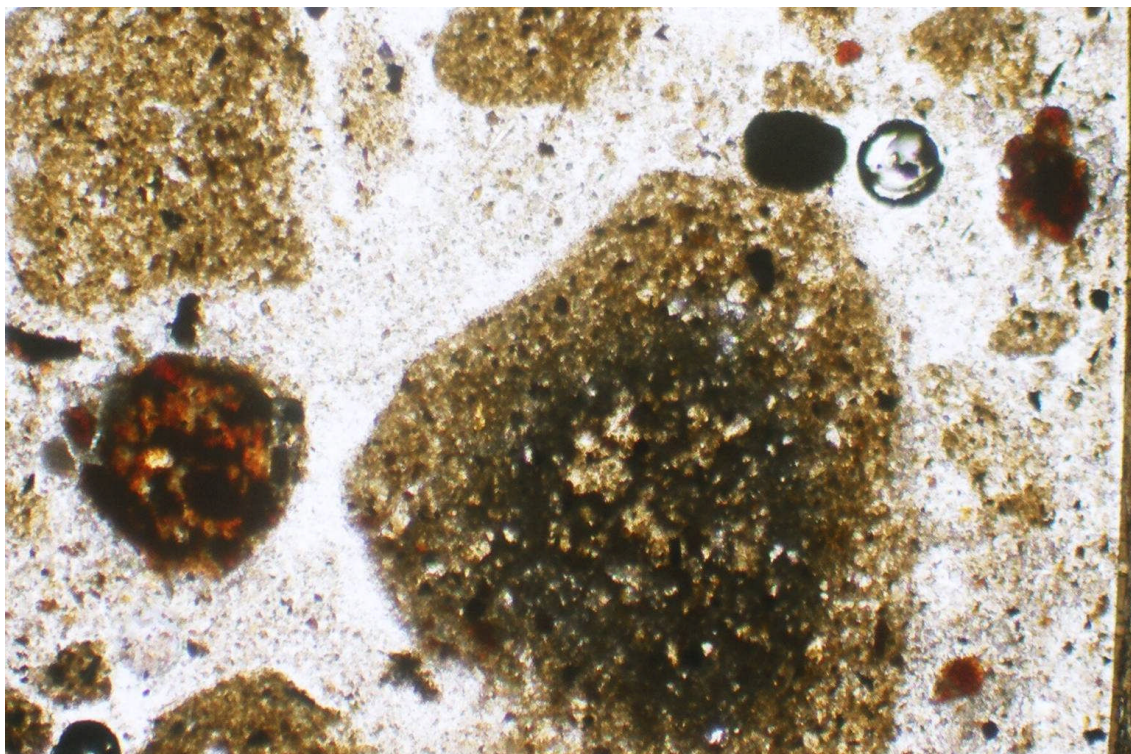
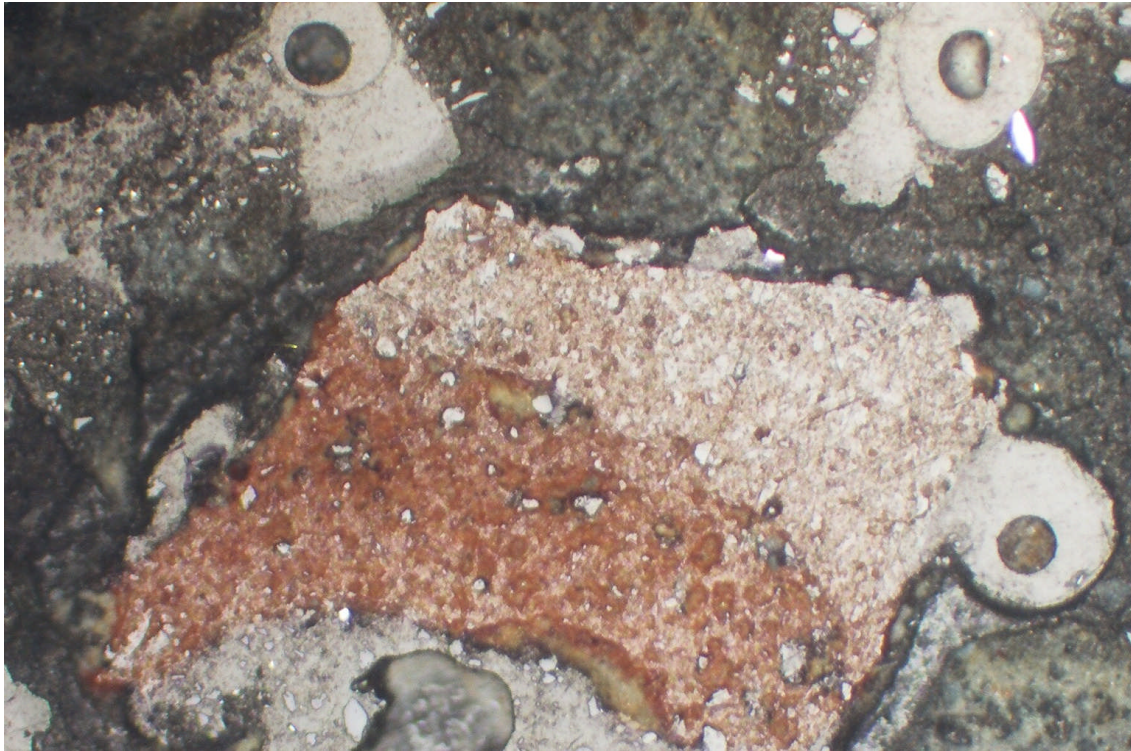


Figure 6. Sample 004A in plain reflected light (top) and in plain transmitted light (bottom), width of field 1.3 mm. The upper photo shows a large fragment of banded (layered) Fe oxyhydroxide. The lower photo shows the turbid, fine-grained character of the tailings, and on the left, a circular particle of reddish Fe oxyhydroxide. Spectra for the oxyhydroxide particles are in Figure 7.

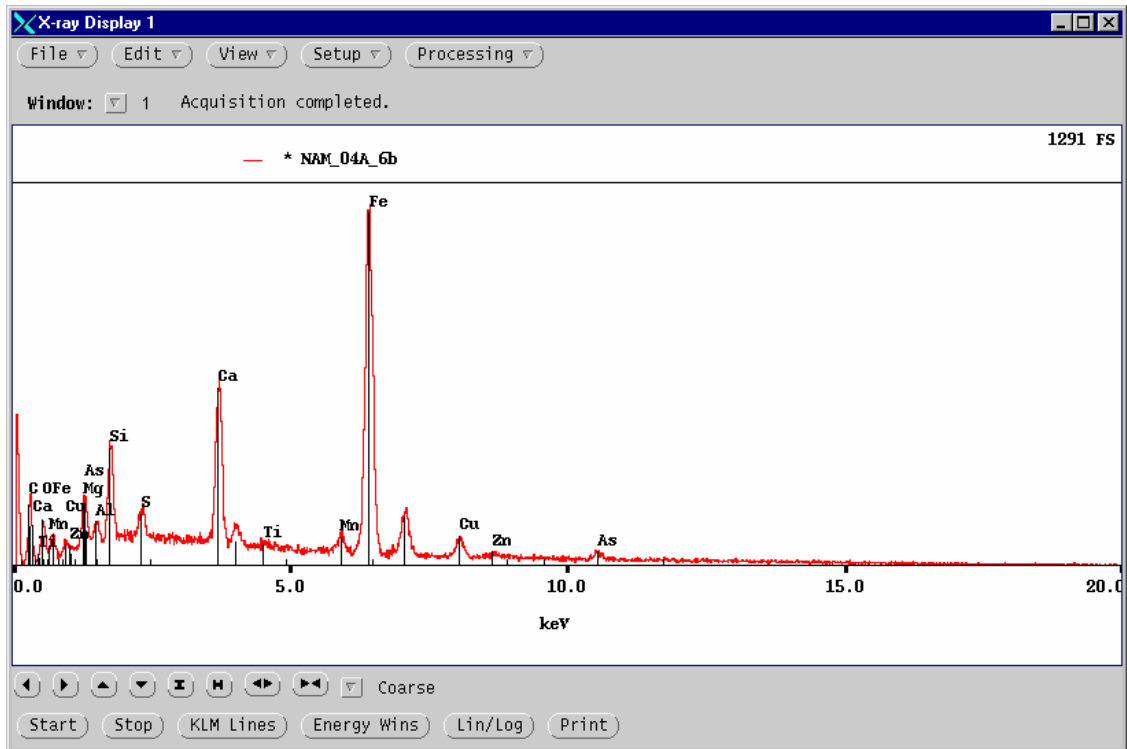
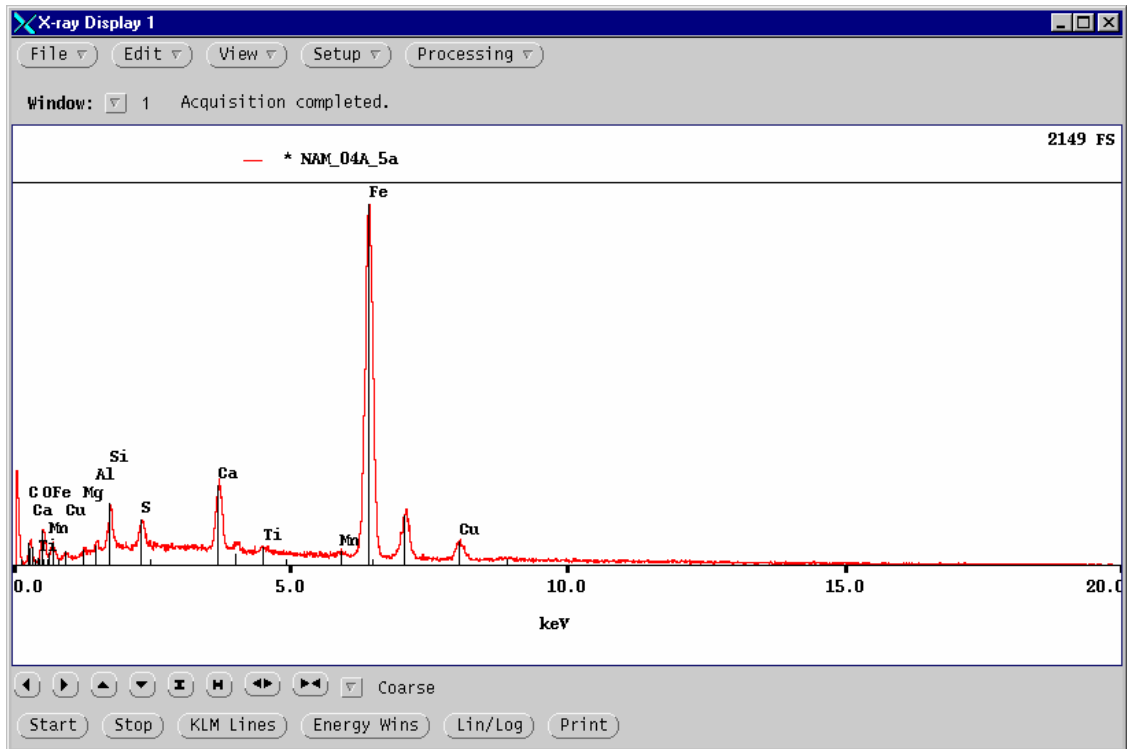


Figure 7. EDS spectra of the Fe oxyhydroxides in the upper and lower photos, respectively, of Figure 6.

Sample 004B

Sample 004B is representative of the coarser portion of sample 004. The polished thin-section megascopically contains more reddish Fe oxyhydroxide than does 004A, and a few of the oxyhydroxide particles are almost black. Transmitted-light microscopy revealed that, aside from fragments of Fe oxyhydroxide, the largest particles are quartz. Quartz and a carbonate mineral or minerals make up the bulk of the sample. The carbonate mineral does not occur as coarse grains, and most is present as matrix-like fines with muscovite. Gypsum is common both as single grains and as aggregates that cement the tailings. SEM-EDS examination of the surficial blebs on the saved intact specimen of 004 indicated that those too are gypsum.

Reflected-light microscopy showed that many of the pyrite grains in 004B are up to 50 μm across, but the overall sulfide-mineral content is nonetheless similar to that of 004A. Several of the pyrite grains have well-developed alteration rims of Fe oxyhydroxide (Figs. 8, 10, 15). A few grains of arsenopyrite [FeAsS] and sphalerite, and one of secondary covellite [CuS], are present; however, despite the relatively high Cu content of the Fe oxyhydroxides, no chalcopyrite [CuFeS₂] was observed in 004A or 004B.

The sample was chosen for a quantitative mineralogical determination because it was considered to provide the best opportunity to establish the identity of the Fe oxyhydroxides. The results (Appendix 1) indicate that the carbonate mineral is calcite and that goethite [α -FeO(OH)] is below the detection limit. A specific search was made for ferrihydrite [nominally 5Fe₂O₃·9H₂O] but it was not detectable. Although the bulk of the Fe oxyhydroxide may therefore be presumed to be amorphous, the presence of at least some ferrihydrite cannot be discounted; the mineral has extremely poor X-ray diffraction qualities and would be difficult to detect because of that property when combined with a relatively low percentage in a complex bulk assemblage. A noteworthy feature is that a small amount (0.6 wt%) of jarosite [KFe₃(SO₄)₂(OH)₆] was determined to be present in the sample.

The character of the alteration rims on pyrite, and the results of EDS analyses of the rims and of the fragmental-type Fe oxyhydroxides are given in Figure 8 to 13. The results show the same pattern that was detected on 004A. The fragmental oxyhydroxide is typically Ca- and Cu-rich; however, the Ca but not the Cu contents decrease as the oxyhydroxide becomes increasingly opaque, thus indicating that the Cu is associated with the oxyhydroxide rather than the Ca-rich phase.

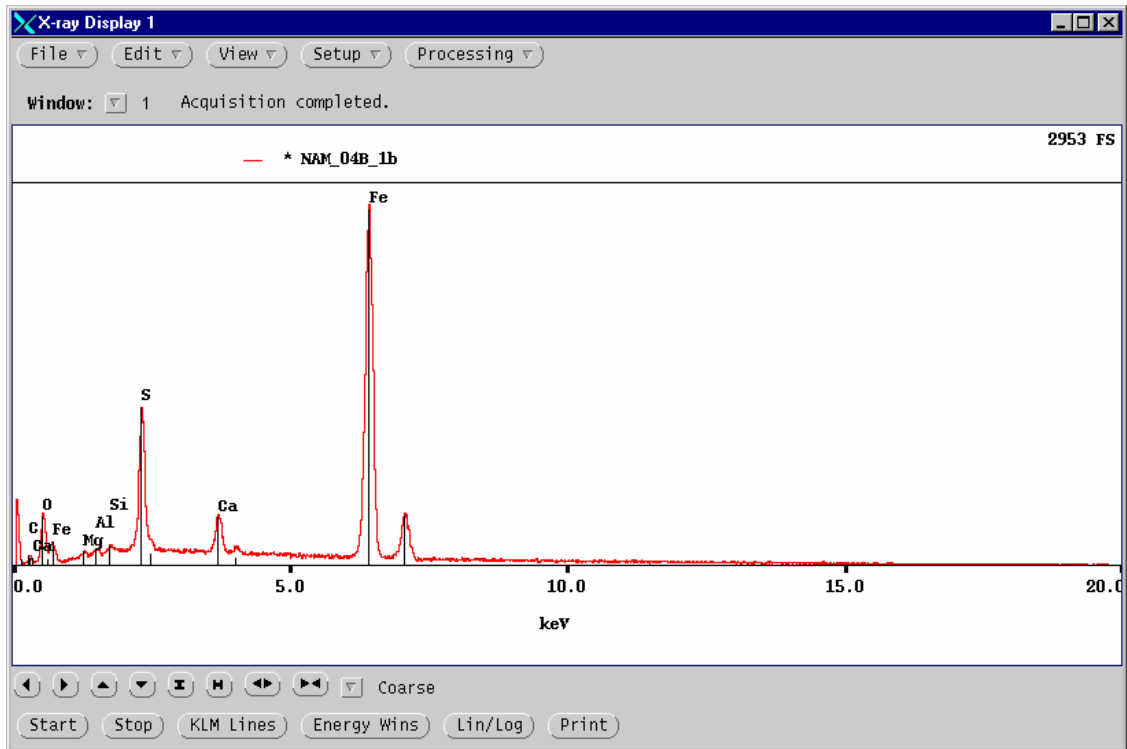


Figure 8. Sample 004B in plain reflected light (top), width of field 0.625 mm, showing two grains of pyrite with grey alteration rims of Fe oxyhydroxide. The EDS spectrum is for the oxyhydroxide associated with the grain at the lower right; a spectrum for the rim on the elongate grain near the centre gave similar results, but with a trace amount of Cu.

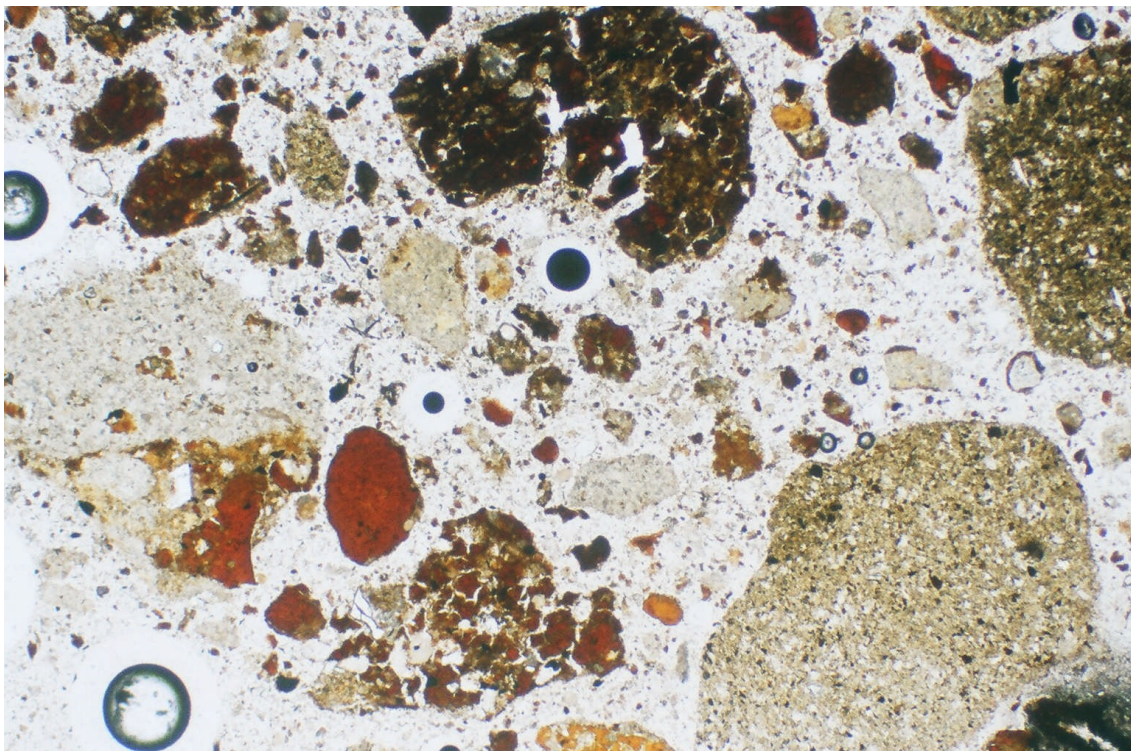
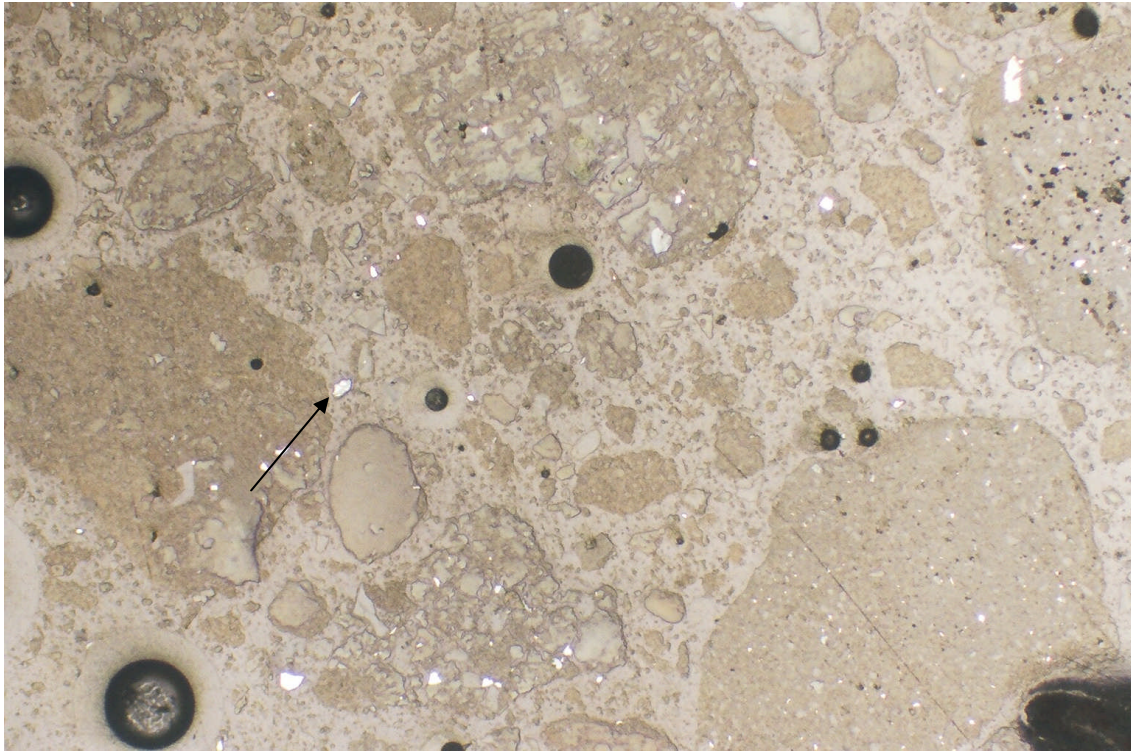


Figure 9. An overview of part of sample 004B in plain reflected light (top), and the same field in plain transmitted light (bottom), width of field 2.6 mm. The white grains in the upper photo are pyrite, and the reddish to almost opaque particles in the lower photo are Fe oxyhydroxide. The arrow points to the altered pyrite grain shown in Figure 10.

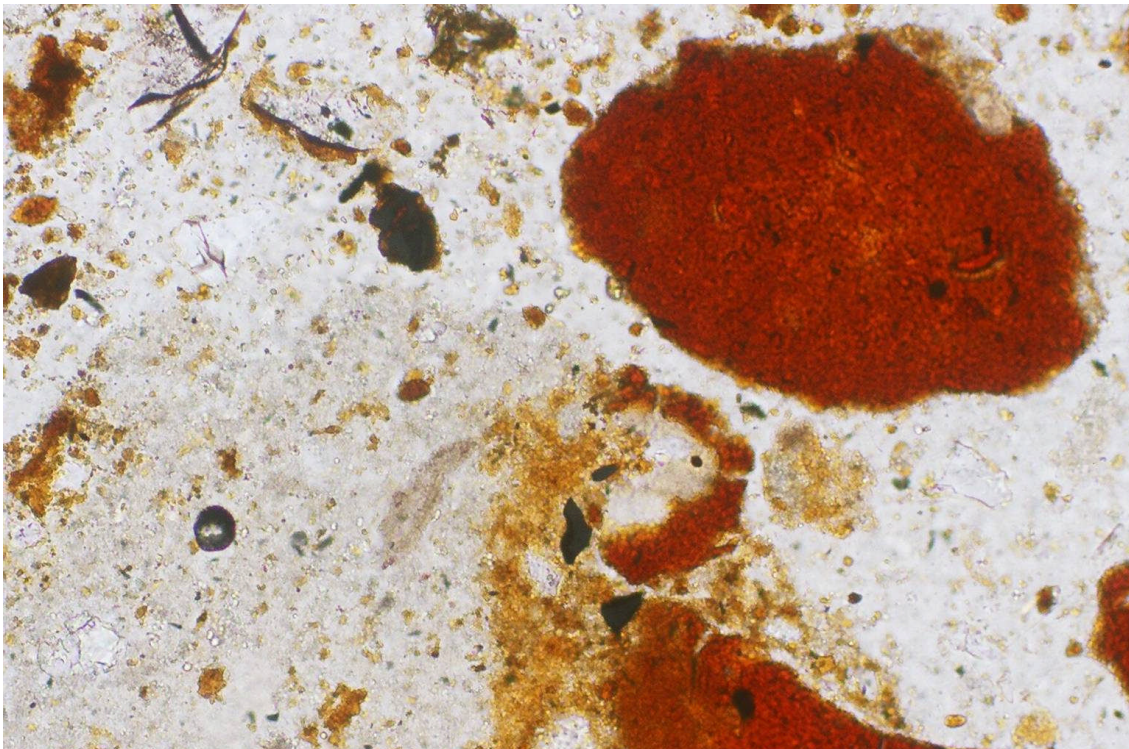
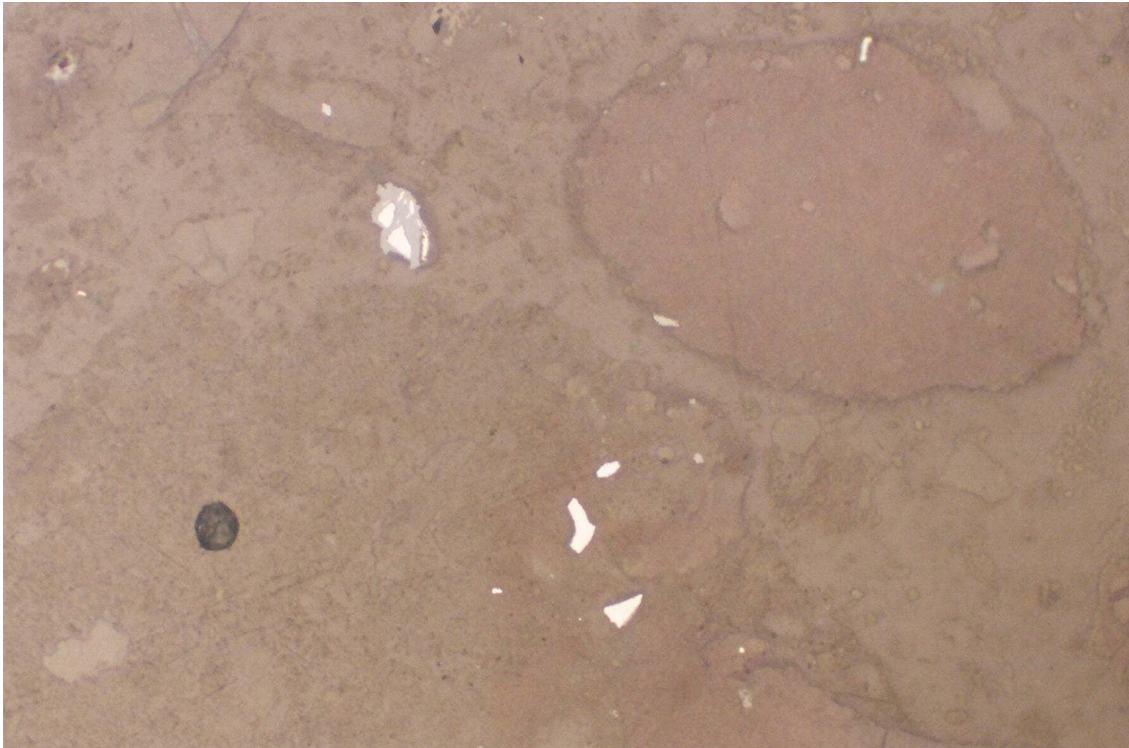


Figure 10. An enlarged part of Figure 9, in plain reflected light (top) and in plain transmitted light (bottom), width of field 0.625 mm. The white grains are pyrite, and the reddish material is Fe oxyhydroxide. EDS spectra for both are in Figure 11.

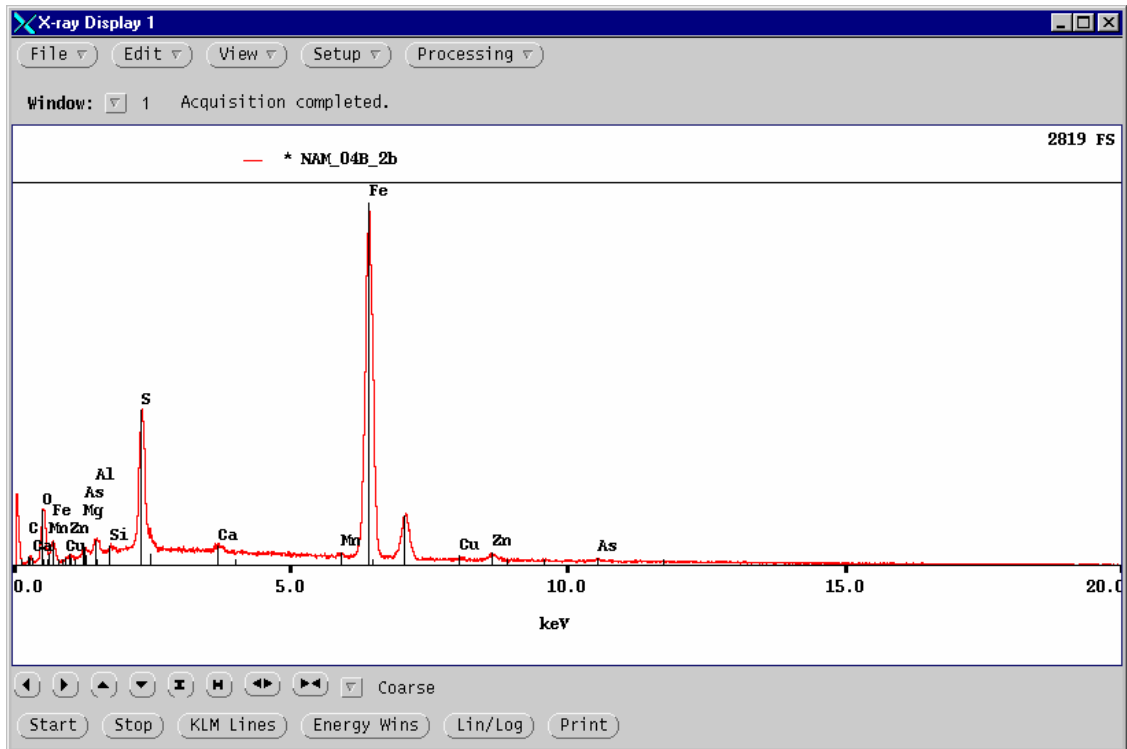
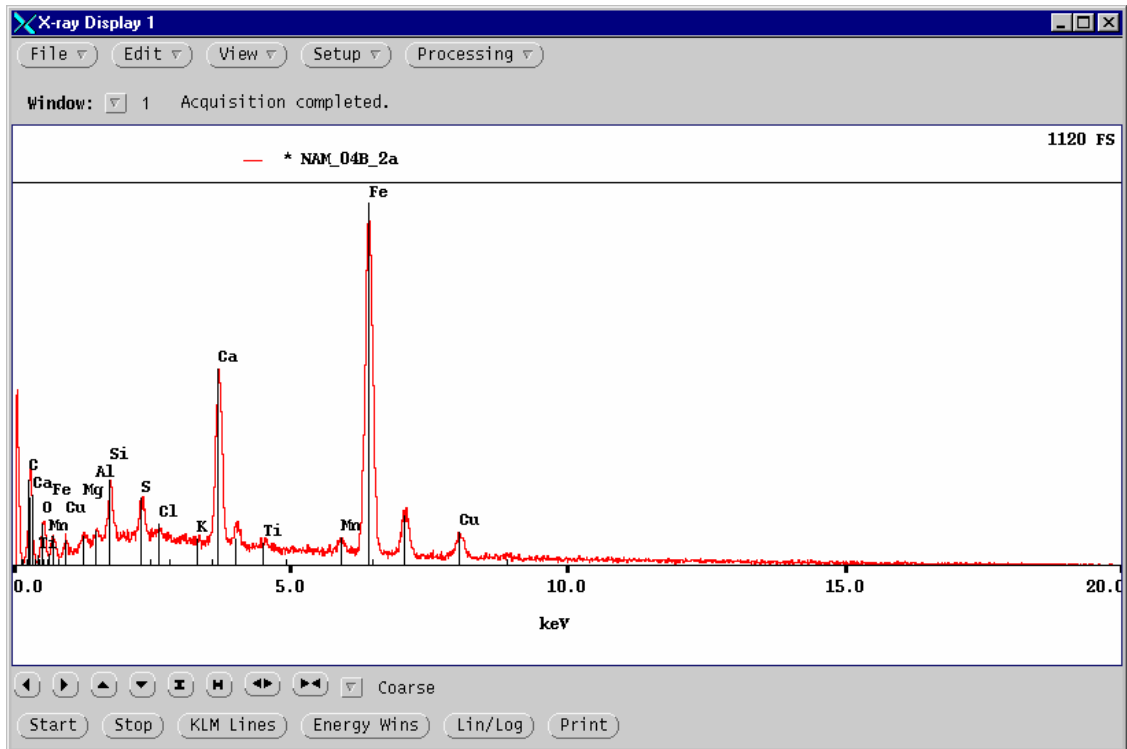


Figure 11. EDS spectra for (top) the large, oval Fe oxyhydroxide at the upper right of Figure 10, and (bottom) for the Fe-oxyhydroxide alteration of pyrite. The spectrum of the fragmental oxyhydroxide is Ca- and Cu-rich whereas the alteration associated with pyrite contains trace amounts of Zn and As.

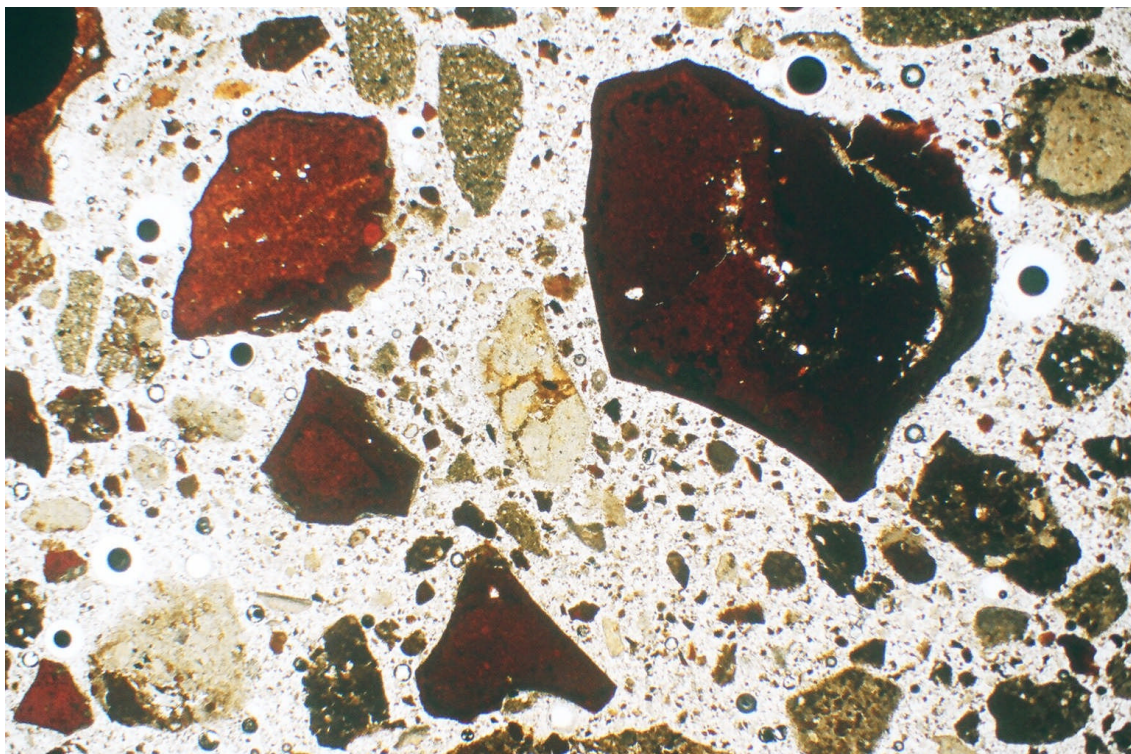
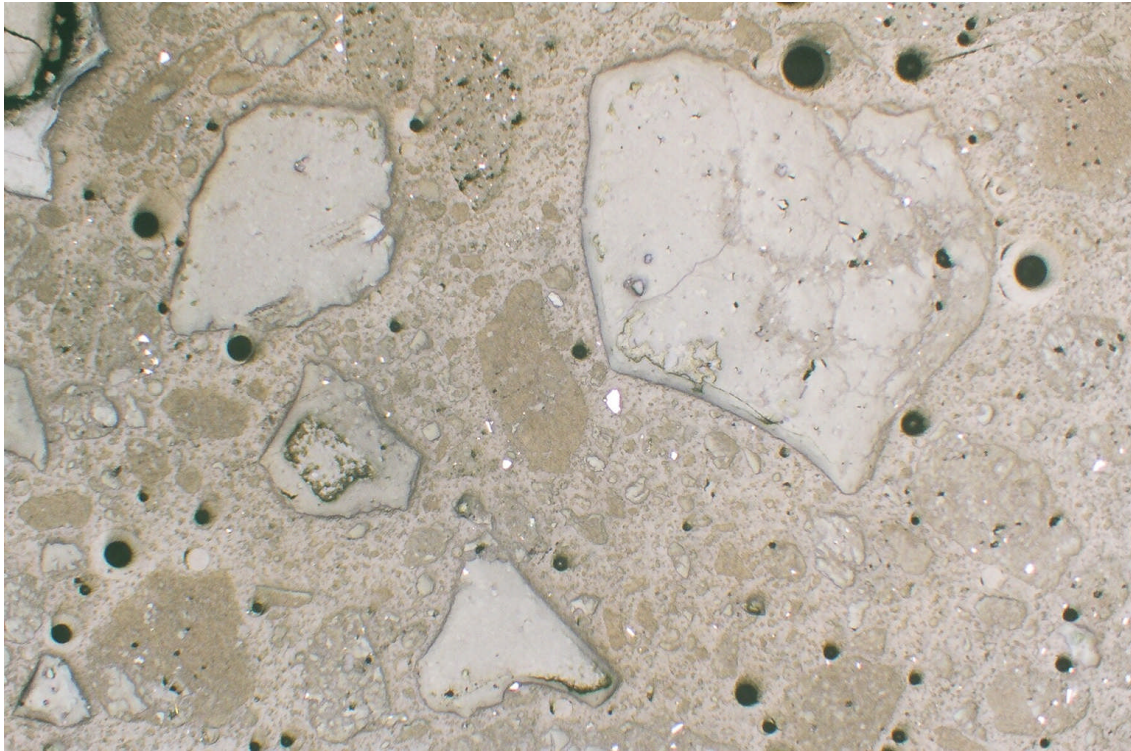


Figure 12. Overview of an area rich in Fe oxyhydroxides in 004B. The upper photo is with plain reflected light, and the lower one is of the same field in plain transmitted light, width of field 5.2 mm. EDS spectra of the largest particle on the left show the typically high Ca and Cu contents whereas the more opaque large particle on the right is much lower in Ca but not Cu.

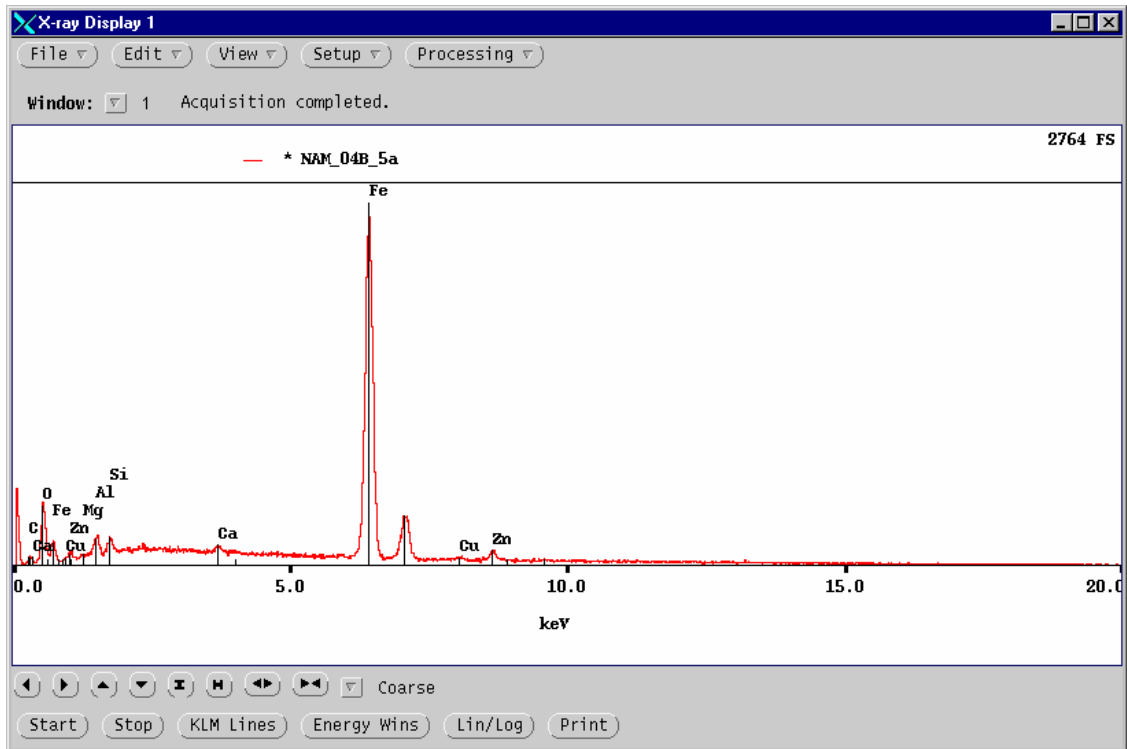


Figure 13. Sample 004B in plain reflected light (top), width of field 0.625 mm. The EDS spectrum is for the broad Fe-oxyhydroxide rim around a core of residual pyrite at the lower left. The upper right quadrant of the photo is fully occupied by a fragment of Fe oxyhydroxide which has the typical high Ca and Cu contents.

Sample 005

The as-received sample was wet and clay-like; its plasticity was pronounced, and the bag had to be slit open because much of the material adhered to the plastic and could not be easily extruded. Despite the wetness of the material, liquid was not present as an isolated phase. The solids were a light grayish brown, but a few ochreous spots, to a maximum of 1½ to 2 mm in diameter, were observed.

The polished thin-section megascopically has a less oxidized appearance than sample 004 insofar as only two or three reddish Fe-oxyhydroxide particles are distinct. Reflected-light microscopy revealed that the section is more sulfide-rich than 004, and the pyrite content was estimated to be ~3%. Pyrite grain sizes are typically <50 µm across. Several grains of sphalerite and of arsenopyrite are present. As well, a few grains of chalcopyrite, trace amounts of galena and secondary covellite (the largest grain of the latter is ~7 × 20 µm), and one particle of polycrystalline marcasite [FeS₂] about 30 µm across, were observed. One of the grains of sphalerite has a narrow rim of covellite. Pyrite forms >95% of the total sulfide content, and the relative abundance of the others was estimated to be sphalerite > arsenopyrite > chalcopyrite > covellite.

The non-sulfide assemblage, as in 004, consists largely of quartz and carbonates. The overall appearance in transmitted light is brownish (Fig. 14), but large fragmental Fe oxyhydroxides of the type observed in 004 are rare. Two grains of carbon, the larger one 30 × 200 µm, were noted (Fig. 15); the grains are not intergrown with other minerals or attached to them, and possibly the carbon is of anthropogenic origin.

A few of the pyrite and arsenopyrite grains have narrow oxidation rims, and a well-developed rim on an arsenopyrite grain is shown in Figure 16. The EDS spectrum (Fig. 17) indicates that the rim is a Fe arsenate. An unidentified rim on galena (Fig. 18) is apparently a Cu–Zn sulfate. EDS spectra of the large particles of Fe oxyhydroxide (Figs. 19, 21) indicate that they are As-bearing but, unlike in sample 004, they do not have detectable amounts of Cu (Figs. 20, 22).

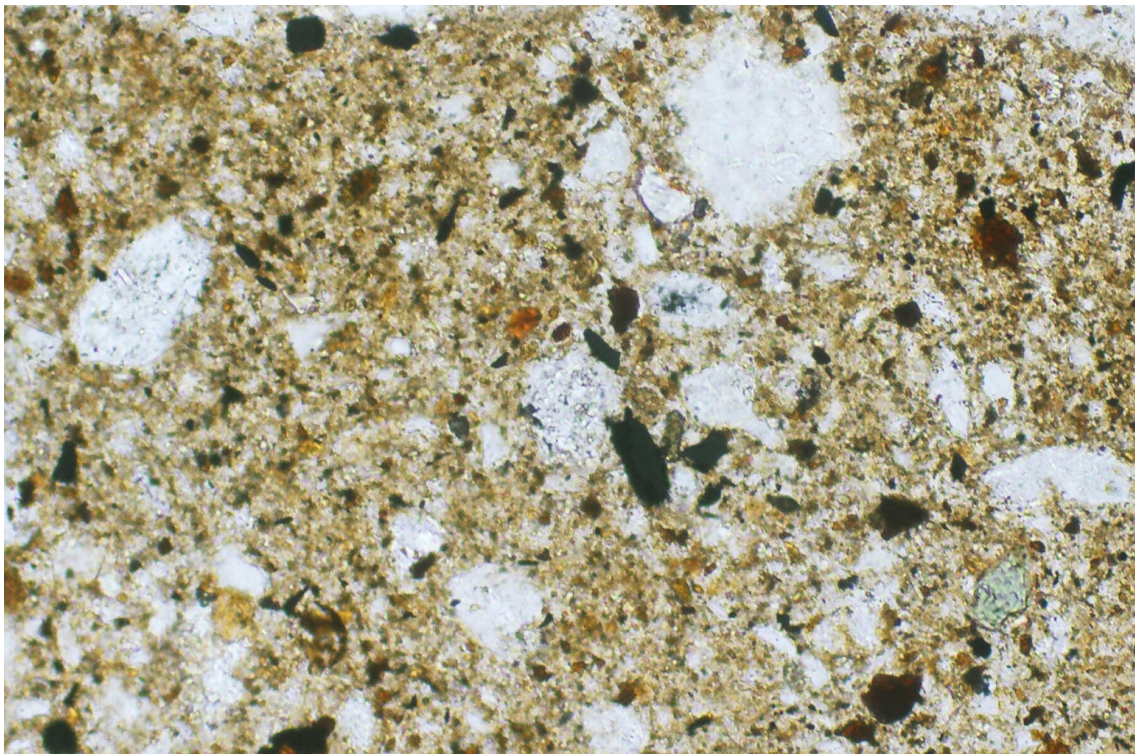


Figure 14. Sample 005 in plain reflected light (top), and the same field in plain transmitted light (bottom) and with polarizers crossed (next page), width of field 0.625 mm. The white grains in the upper photo are pyrite, and the clear grains in the lower photo are mainly quartz.

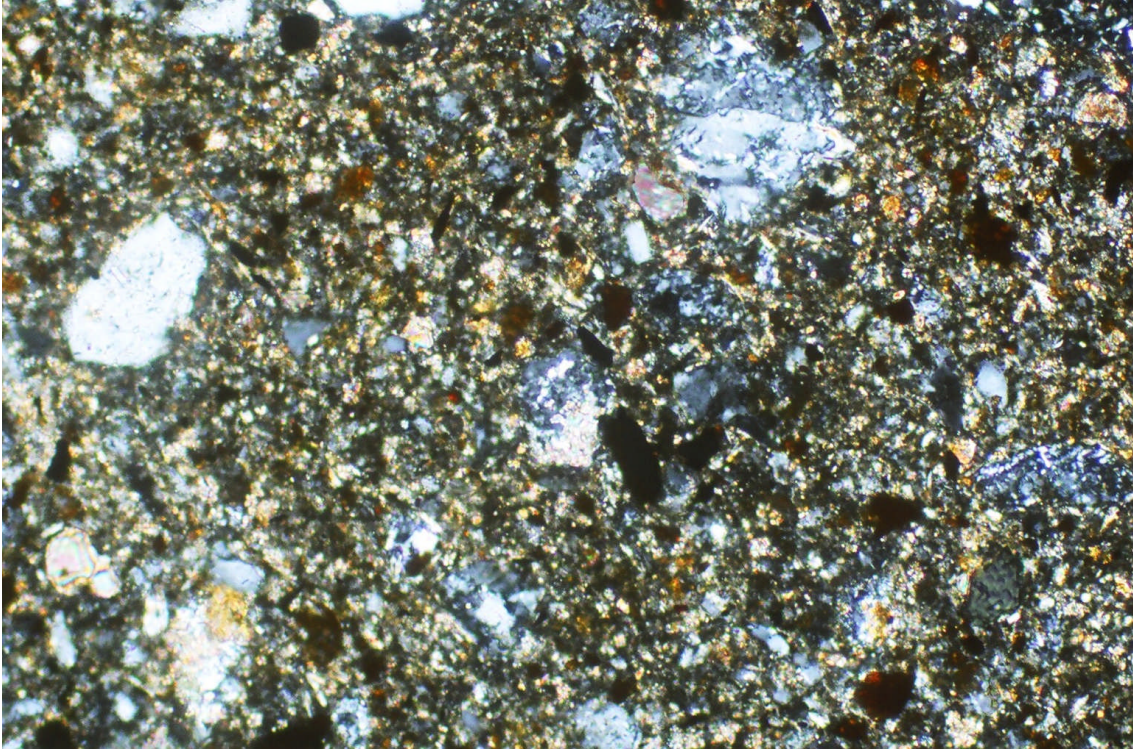


Figure 14 (cont'd). The same field as on the preceding page, but with polarizers crossed. The white to grey grains are mainly quartz, and the coloured grains are mainly carbonate minerals.



Figure 15. Sample 005 in plain reflected light, width of field 0.625 mm. The white grains are mainly pyrite, and the elongate brownish grain above centre is carbon.

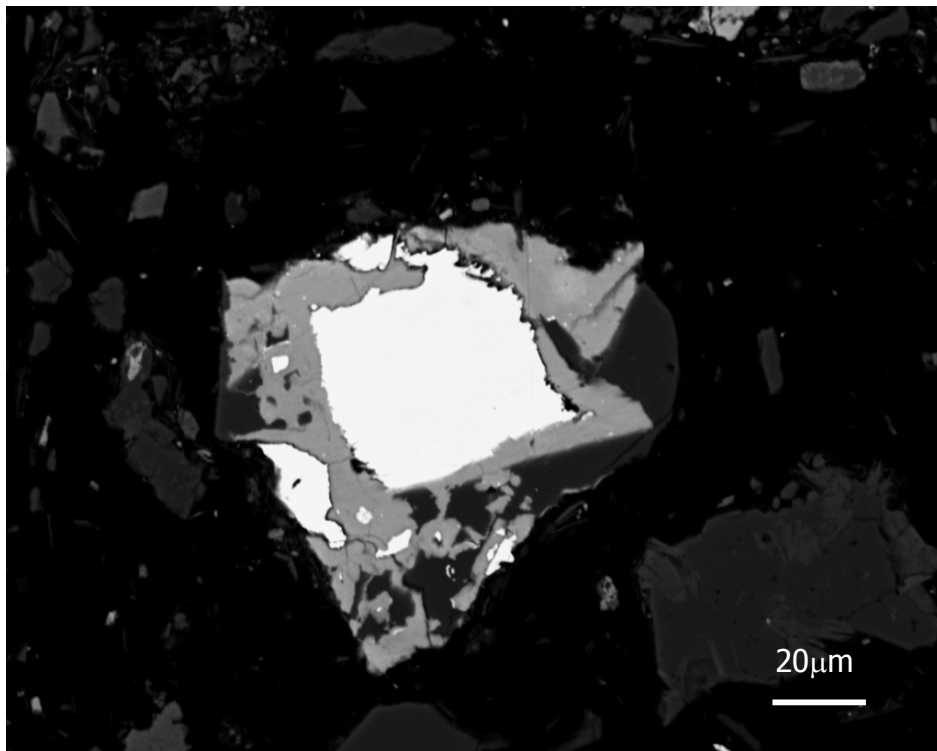
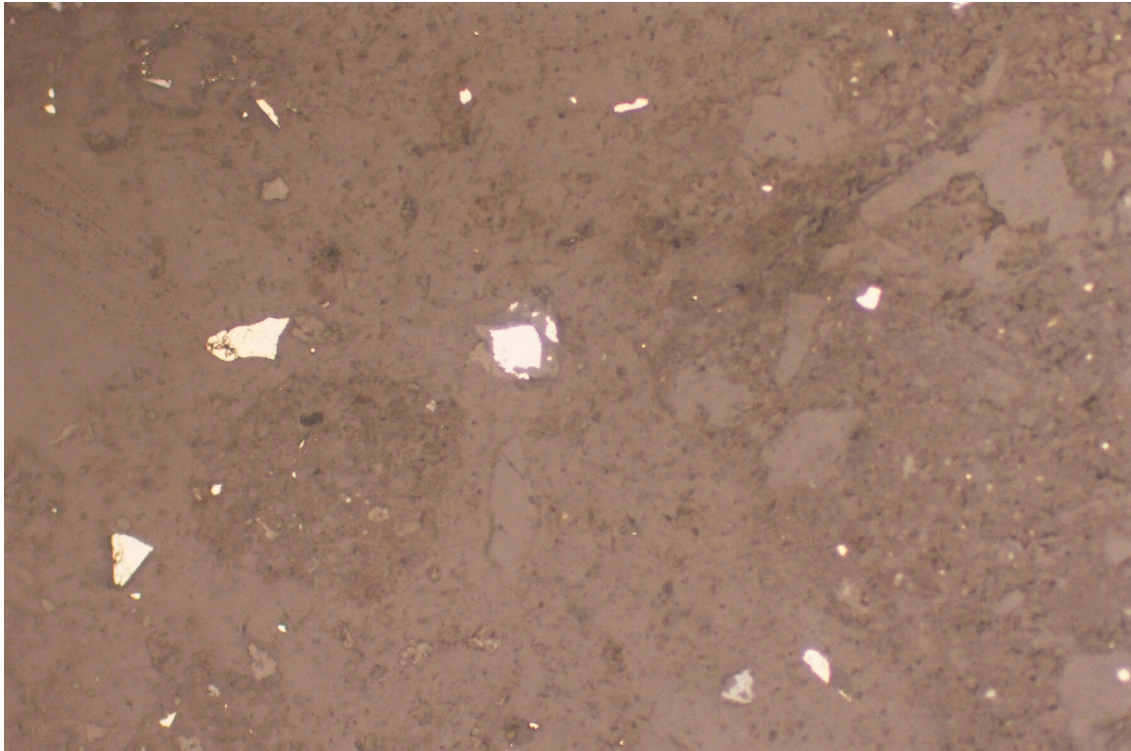


Figure 16. Sample 005 in plain reflected light (top), width of field 0.625 mm. Near the centre is a grain of arsenopyrite with a barely perceptible alteration rim that is readily evident in the backscattered-electron image.

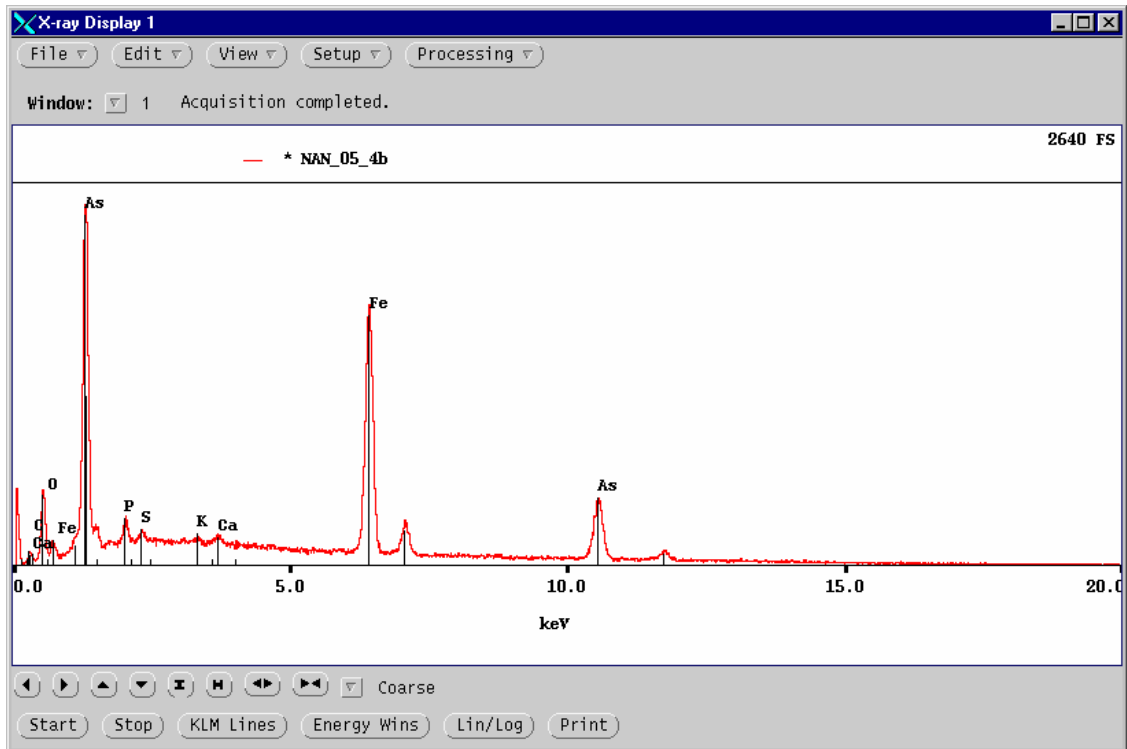


Figure 17. EDS spectrum of the rim on the arsenopyrite grain of Figure 16. The spectrum indicates that the rim is a Fe arsenate.



Figure 18. Sample 005 in plain reflected light, width of field 0.625 mm. To the right of centre is a roughly rectangular bluish grain with a core of galena (white). An EDS spectrum of the outermost rim indicates that the rim is probably a Cu–Zn sulfate.

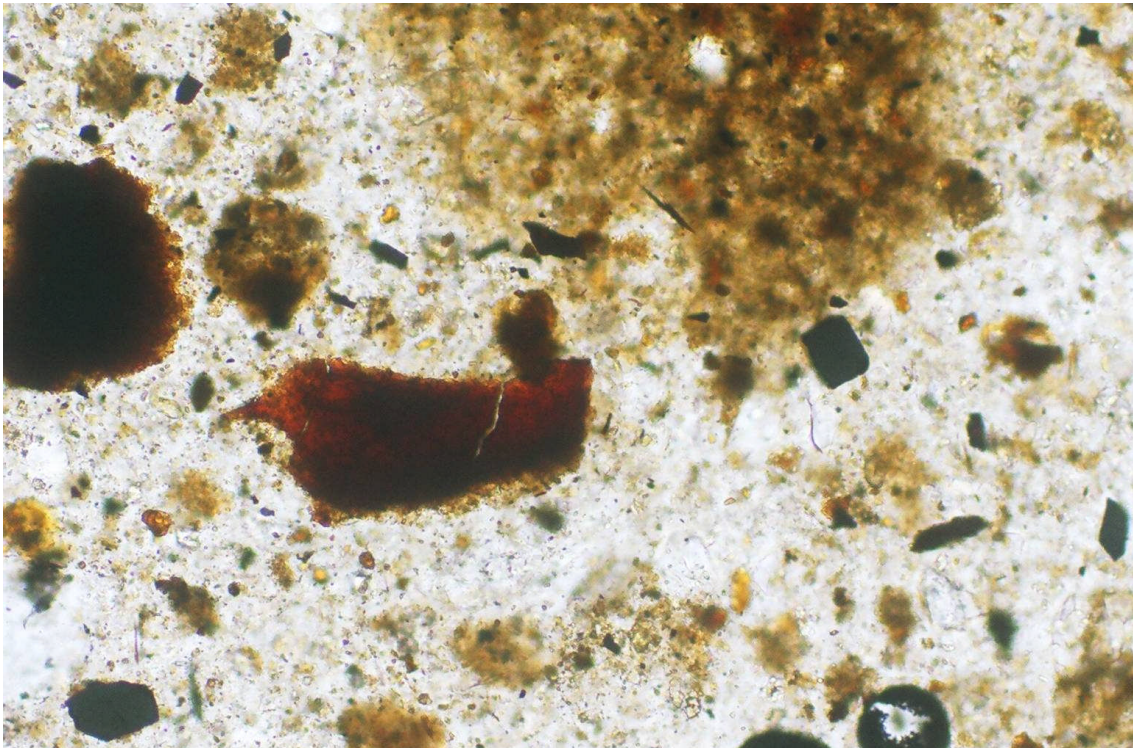
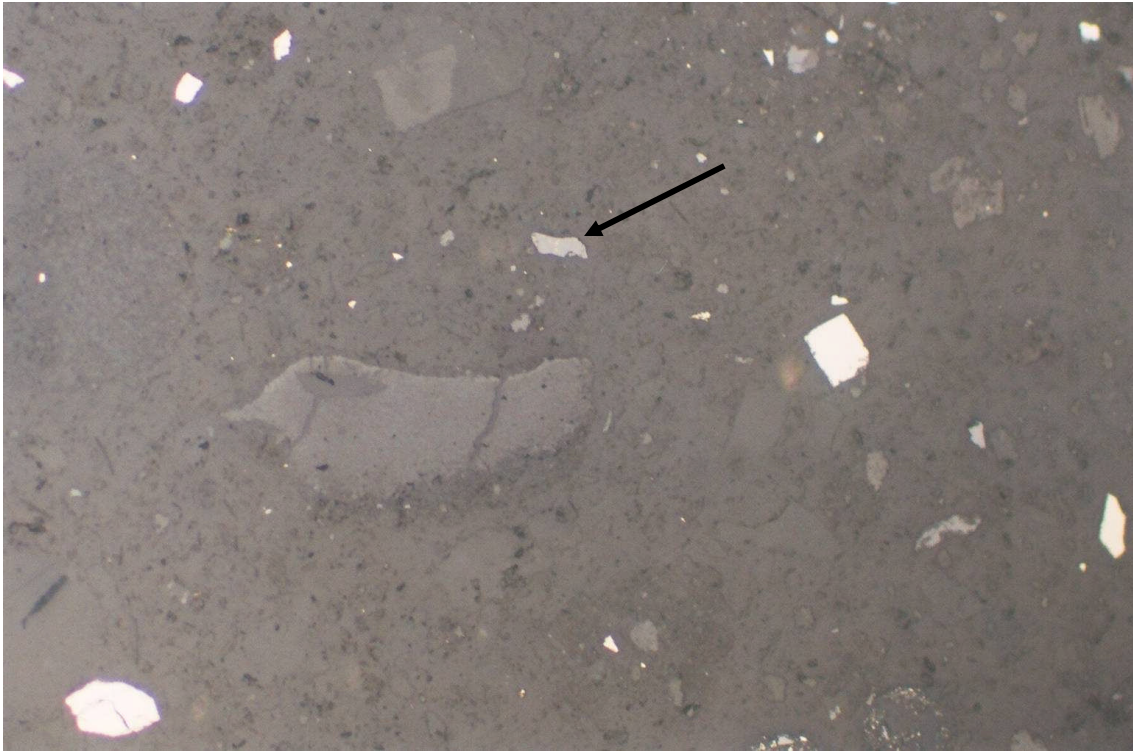


Figure 19. Sample 005 in plain reflected light (top) and in plain transmitted light (bottom), width of field 0.625 mm. The white grains are pyrite, and the arrow points to a grain of sphalerite, beneath which is a large particle of As-bearing Fe oxyhydroxide (Fig. 20).

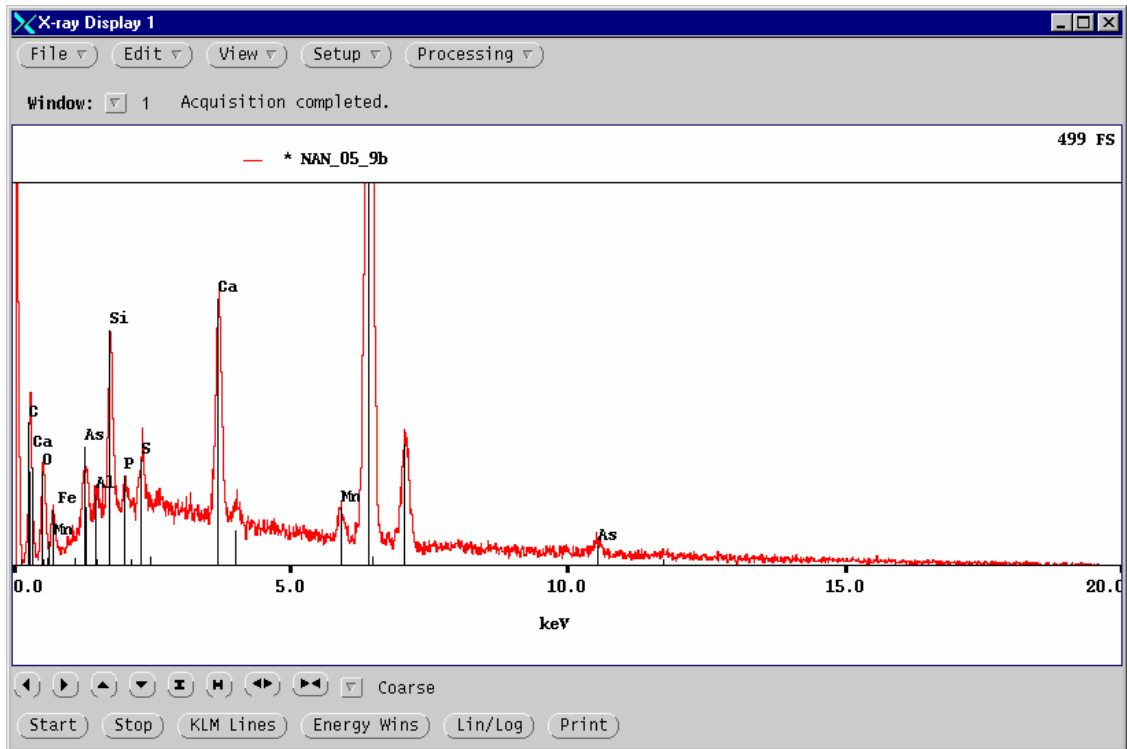


Figure 20. Expanded-scale EDS spectrum of the large particle of As-bearing Fe oxyhydroxide shown in Figure 19.

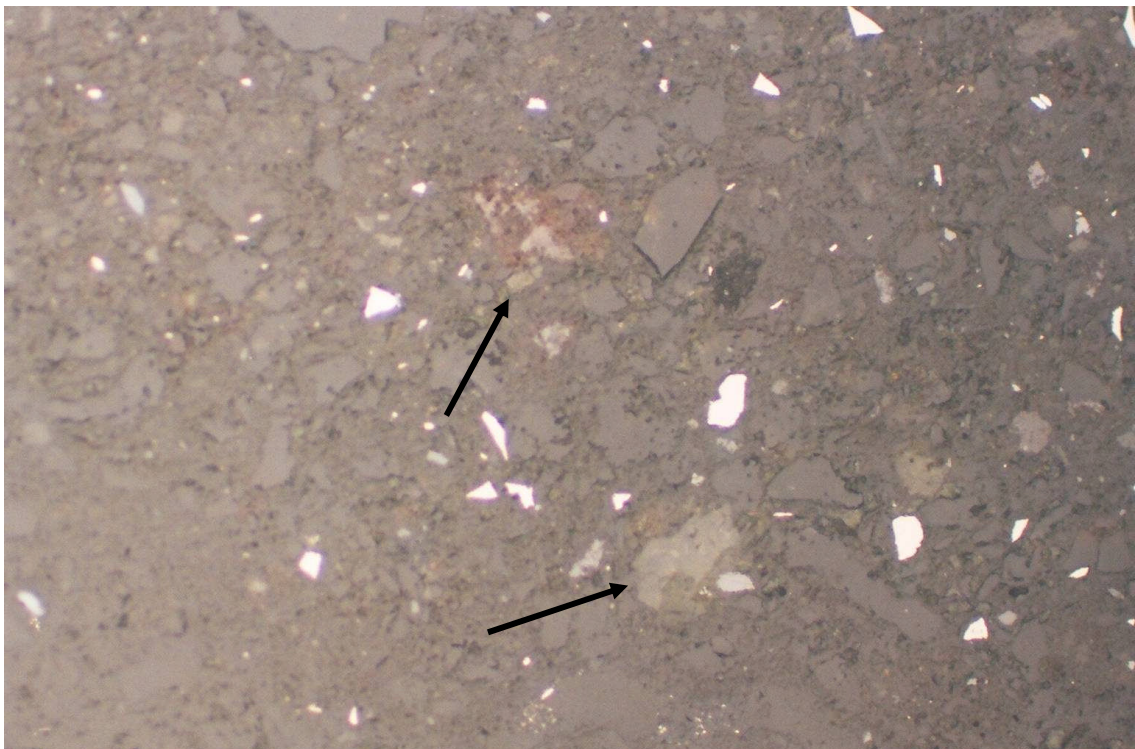


Figure 21. Sample 005 in plain reflected light, width of field 0.625 mm. The white grains are pyrite. The upper arrow points to a reddish particle of As-bearing Fe oxyhydroxide (Fig. 22). The lower arrow points to a large grain of dolomite; the small adjoining, roughly oval, grey grain on the right is sphalerite.

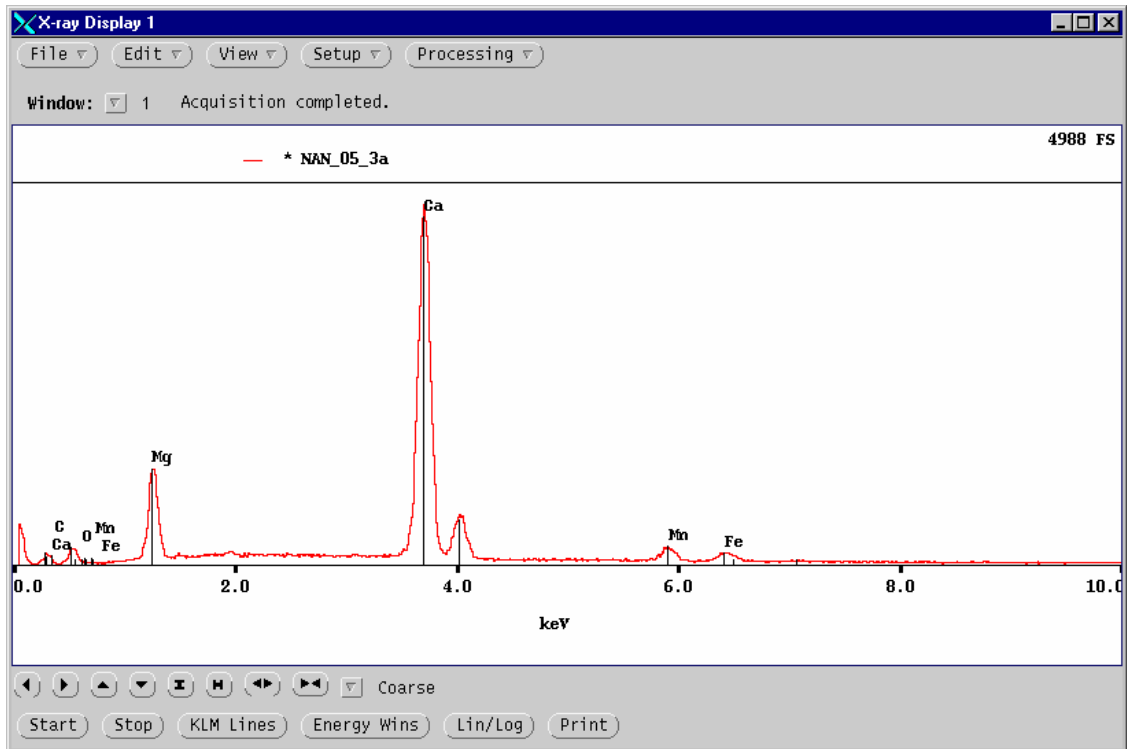
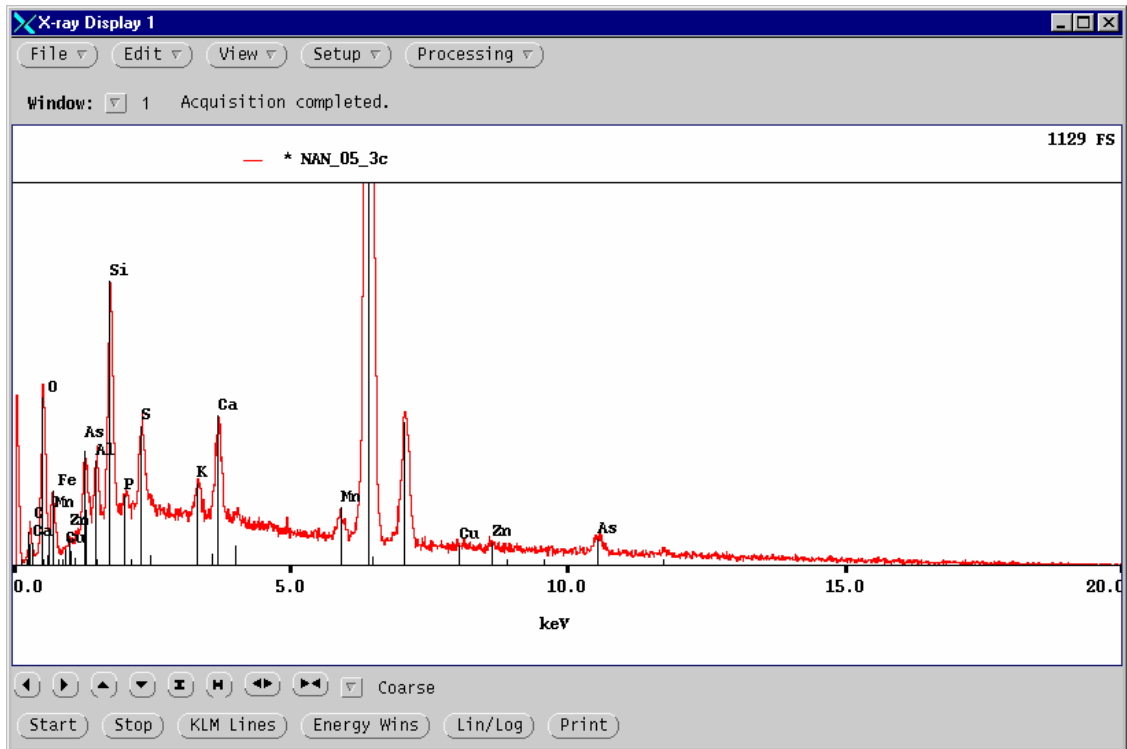


Figure 22. EDS spectra of the Fe oxyhydroxide (top) and dolomite (bottom) of Figure 21. The upper spectrum is at an expanded scale to illustrate the presence of As.

Sample 006

The as-received sample was similar in colour to that of 005 but was noted to be slightly coarser grained. About a quarter of the material was observed to be finer grained than the main mass, and only within this finer portion were there sparse spots of ochreous material, each only about 1 mm in diameter. Abundant excess fluid was present, requiring that the sample be ejected into a plastic vessel rather than onto a sheet.

The polished thin-section is megascopically light brown, like that of 005. Only three distinctly reddish particles of presumed Fe oxyhydroxide are present. Very fine-grained sulfides are dispersed throughout the section.

Microscopy in transmitted light revealed that only one of the reddish particles observed megascopically is solid Fe oxyhydroxide, and the others are polishing artifacts. The non-opaque assemblage consists principally of quartz and carbonates. Many of the quartz particles are fine-grained chert-like mosaic intergrowths rather than single grains, but both types are abundant. A few of the carbonate grains are coarse-grained and homogeneous; the grains are variously calcite of end-member composition, and ferroan dolomite. Chlorite and muscovite are present as fine-grained intergrowths with quartz; the chlorite also occurs sparingly as lath-like intergrowths and is more abundant than in sample 005. A few grains of epidote, amphibole, and biotite were observed.

The sulfides are megascopically visible because the grain size of pyrite is commonly up to 100 μm across, and many grains range from 50 to 90 μm . Fewer grains of pyrite than in 005 are present, but the overall content is about the same because of the larger size of the grains in 006. Chalcopyrite, arsenopyrite, and sphalerite occur sparingly. Oxidation rims on pyrite are more common and are broader than in 005 (Fig. 23), and a distinct feature is that several of the Fe-oxyhydroxide particles appear to be pseudomorphs after pyrite.

Numerous EDS spectra were obtained for the alteration rims and for isolated Fe-oxyhydroxide particles (Figs. 25-32). Many of the particles and rims contain trace amounts of Cu and (or) Zn, and some have detectable As. One of the particles has a composition corresponding to that of plumbojarosite $[\text{PbFe}_6(\text{SO}_4)_4(\text{OH})_{12}]$; Fig. 31].



Figure 23. Sample 006 in plain reflected light, width of field 0.625 mm, showing Fe-oxyhydroxide rims on pyrite. The adjacent white prismatic grain southeast of the altered pyrite in the upper photo is arsenopyrite, as is the elongate white grain in the lower photo.

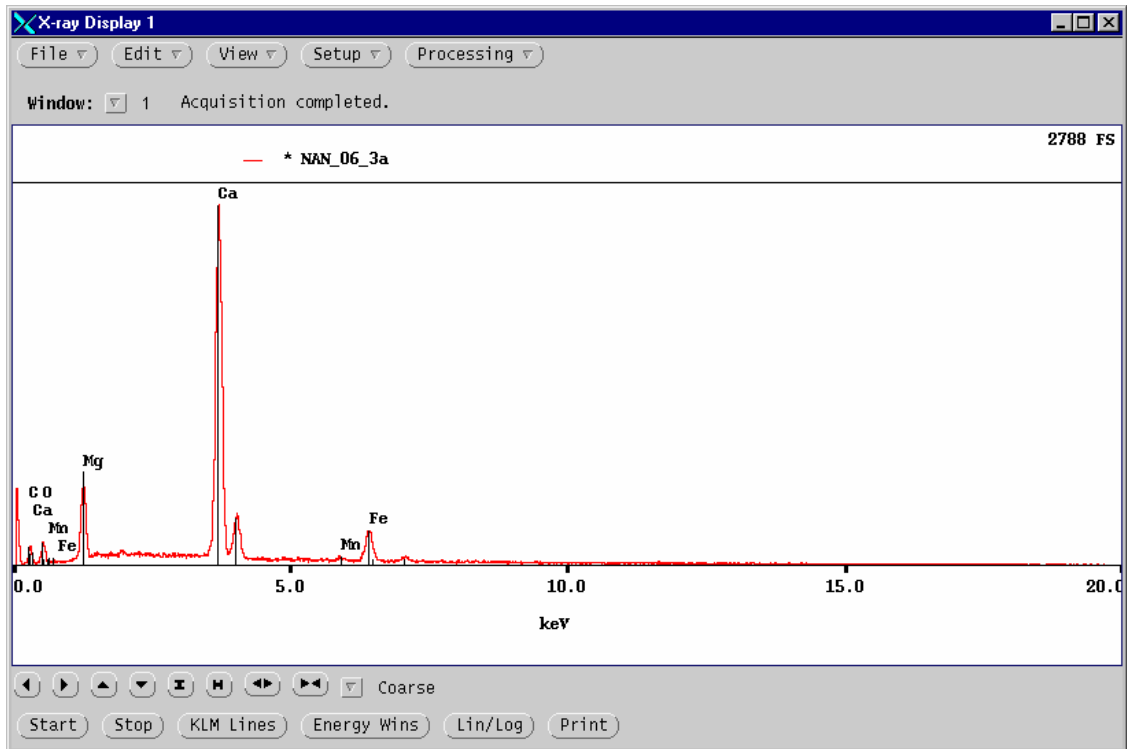
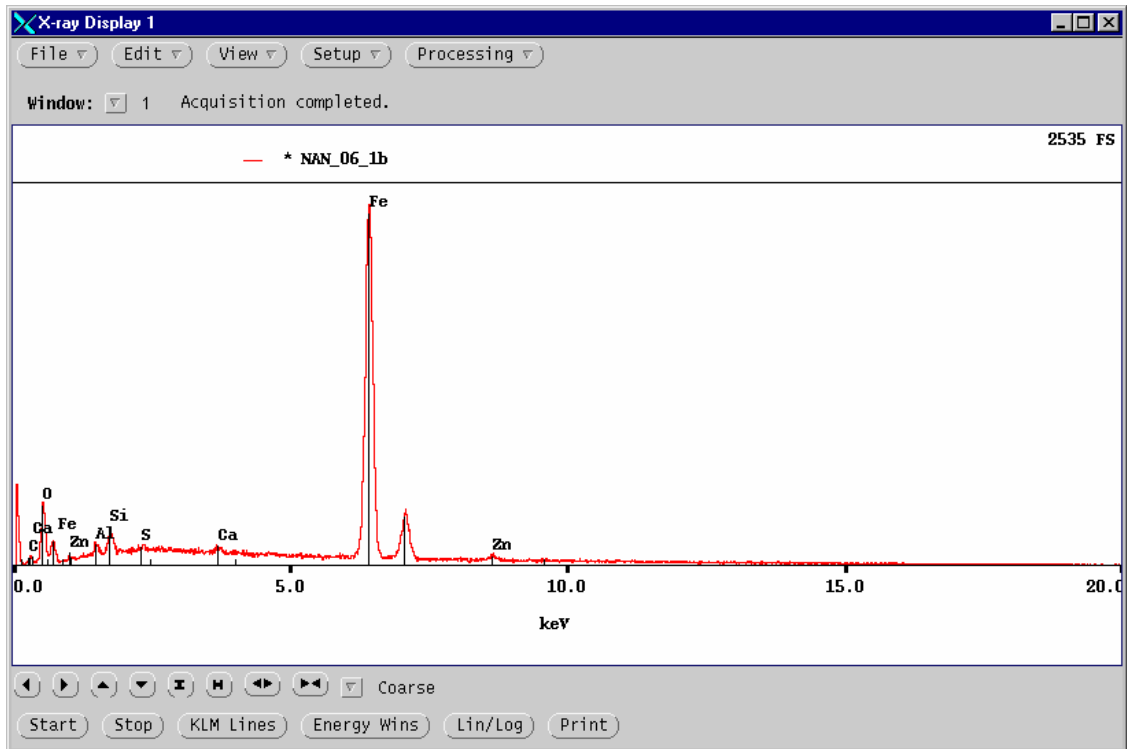


Figure 24. EDS spectrum of the Fe-oxyhydroxide rim on pyrite in the upper photo of Figure 23. The rim on the grain in the lower photo gave a similar spectral result. The lower spectrum is of the large dolomite grain showing cleavage traces at the northeastern corner of the lower photo in Figure 23.



Figure 25. Sample 006 in plain reflected light, width of field 0.625 mm, showing Fe-oxyhydroxide alteration of pyrite. An EDS spectrum of the oxyhydroxide in the upper photo showed the presence of trace Zn, but no heavy metals were detected in the oxyhydroxide in the lower photo.

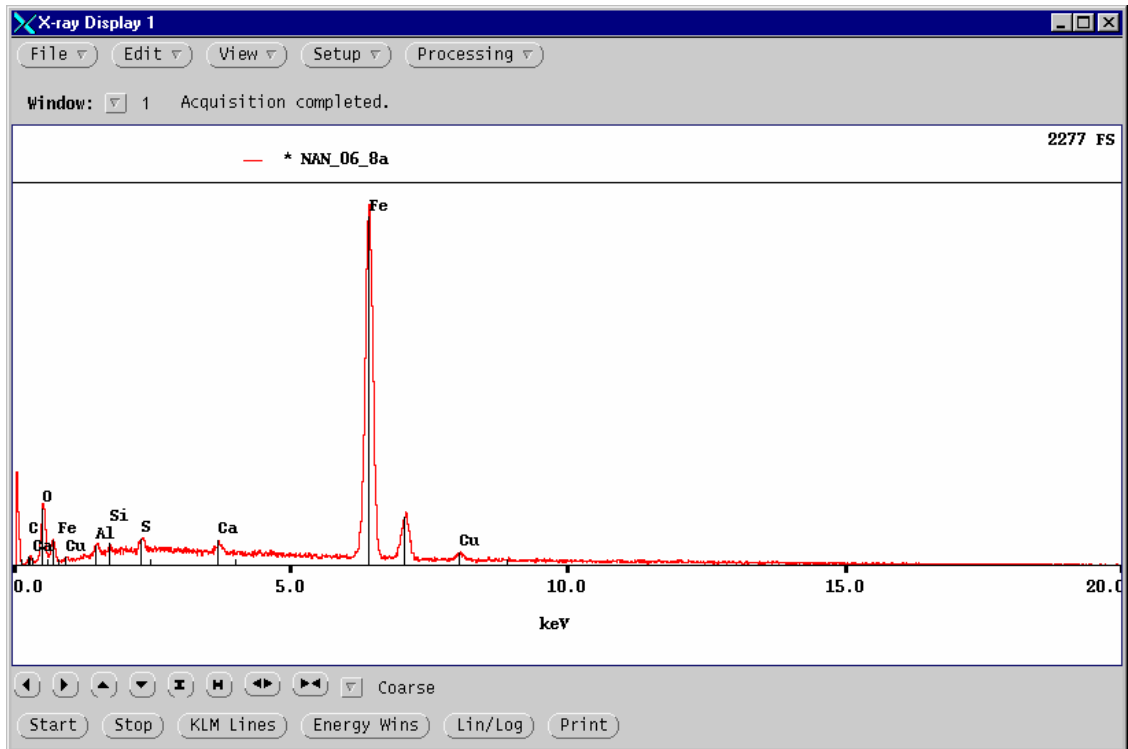
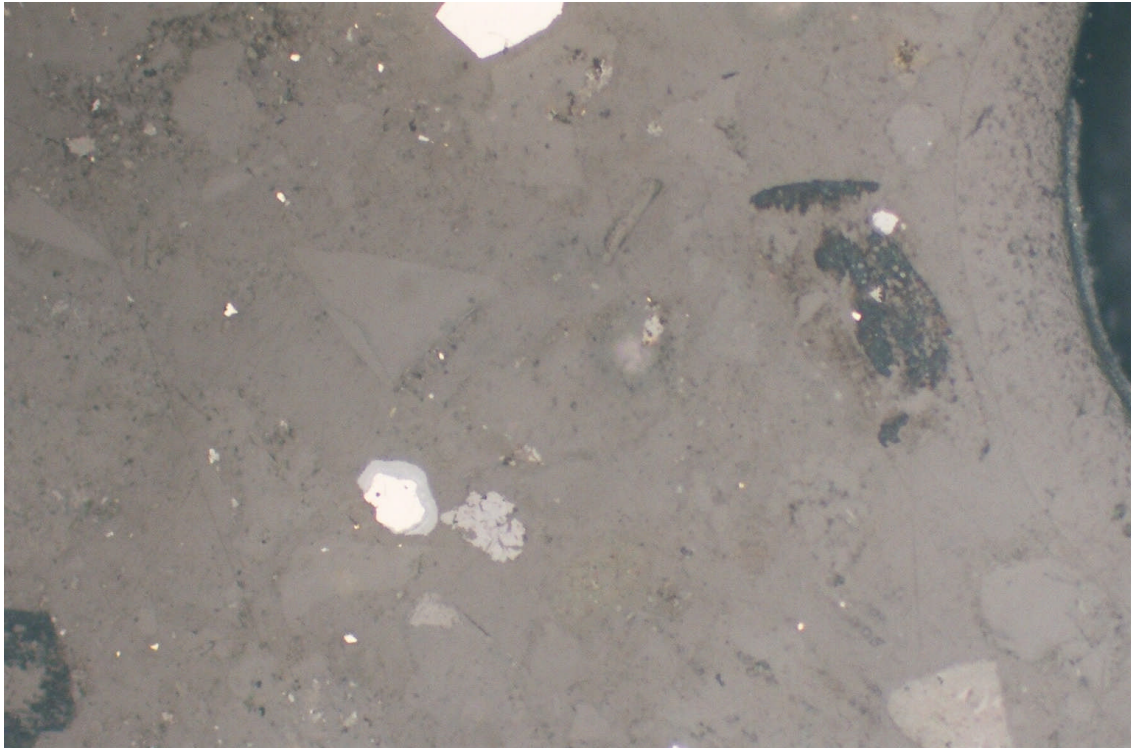


Figure 26. Sample 006 in plain reflected light, width of field 0.625 mm, showing a Fe-oxyhydroxide rim on pyrite, and the EDS spectrum for the rim.

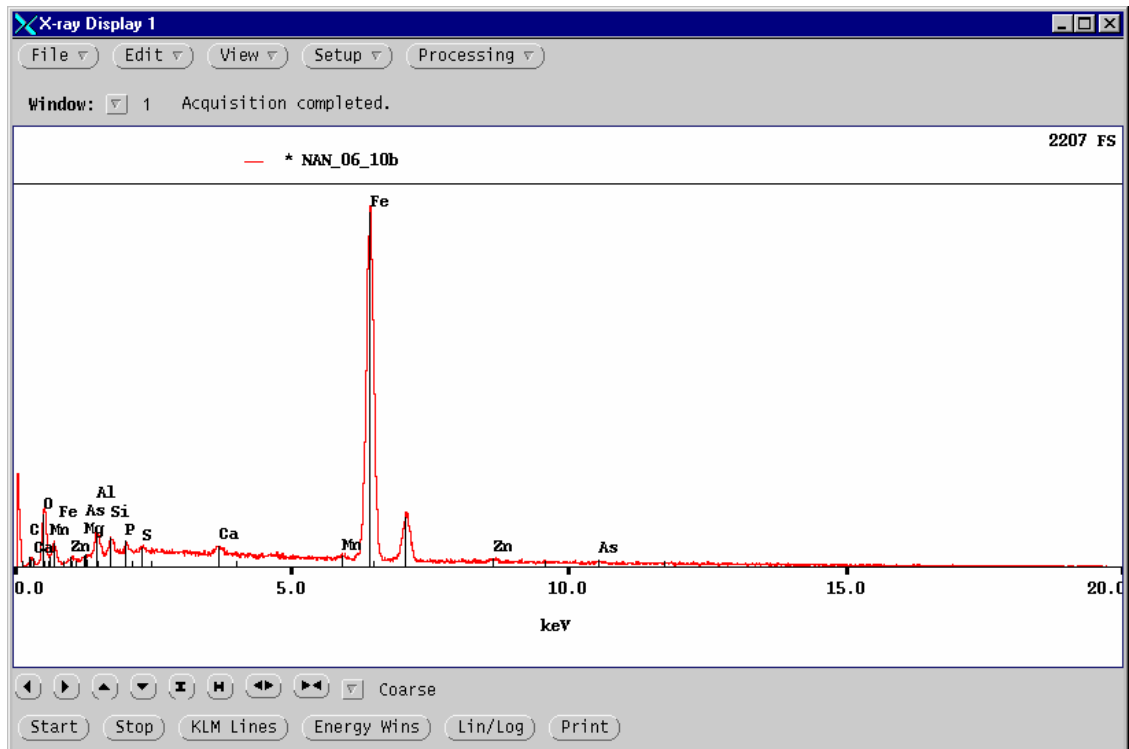
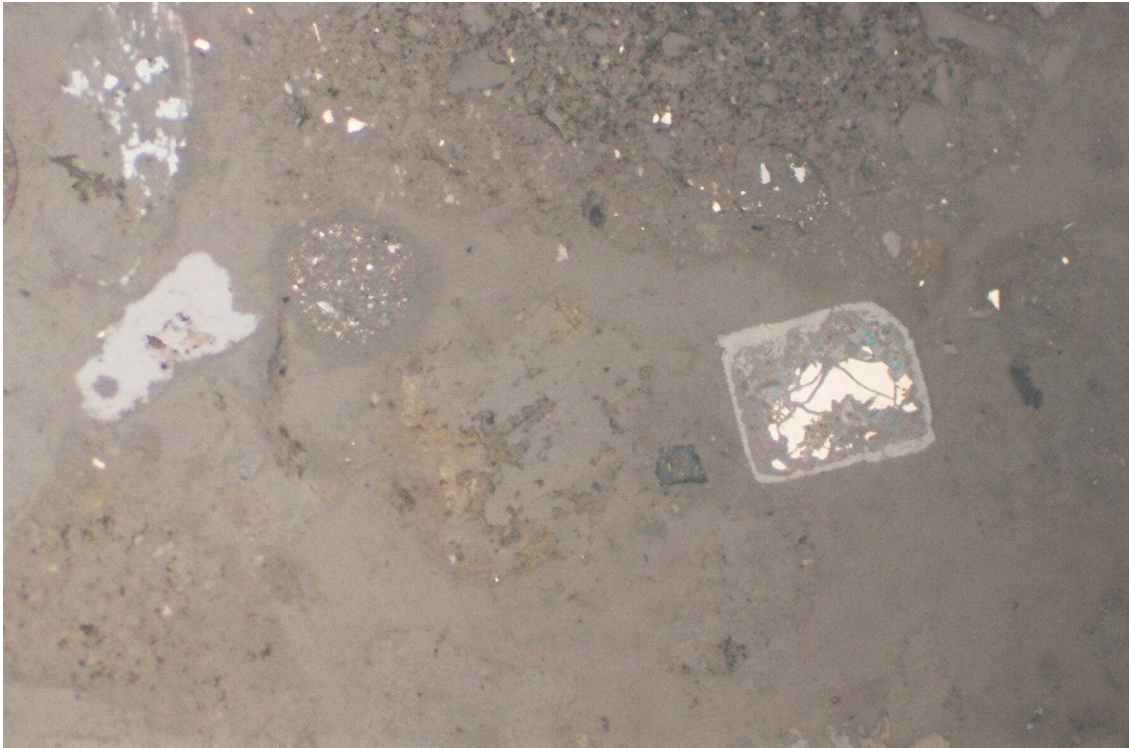


Figure 27. Sample 006 in plain reflected light, width of field 0.625 mm, showing residual pyrite and secondary covellite (blue) enclosed within an outer rim of Fe oxyhydroxide, for which the EDS spectrum is shown (trace Zn only). The large grey particle at the far left, mid-height, is also relatively pure Fe oxyhydroxide, but it contains a trace amount of As.

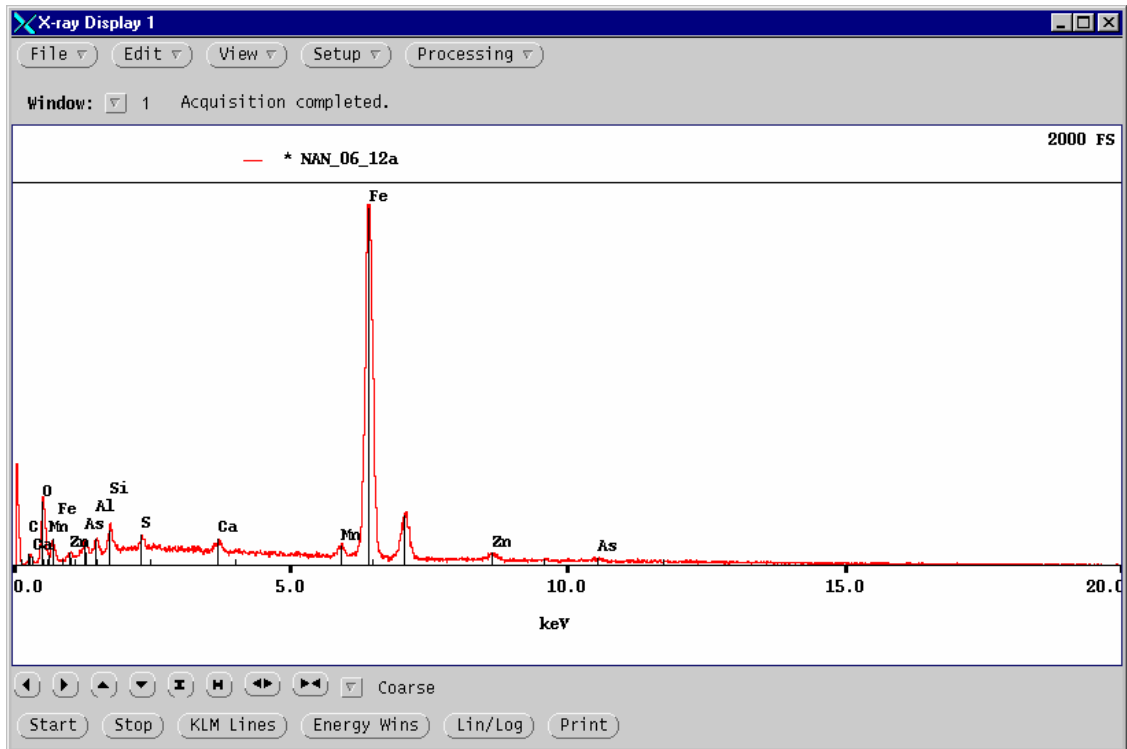


Figure 28. Sample 006 in plain reflected light, width of field 0.625 mm, showing residual pyrite within Fe oxyhydroxide that the EDS spectrum indicates to be Zn- and As-bearing.

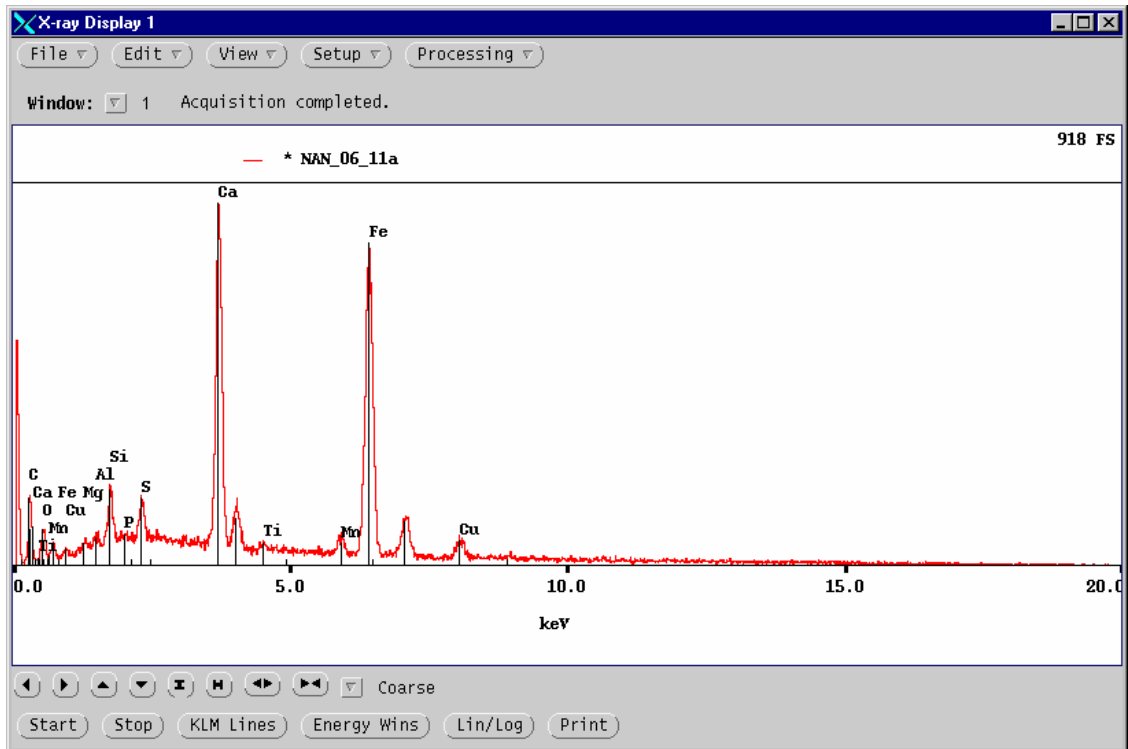
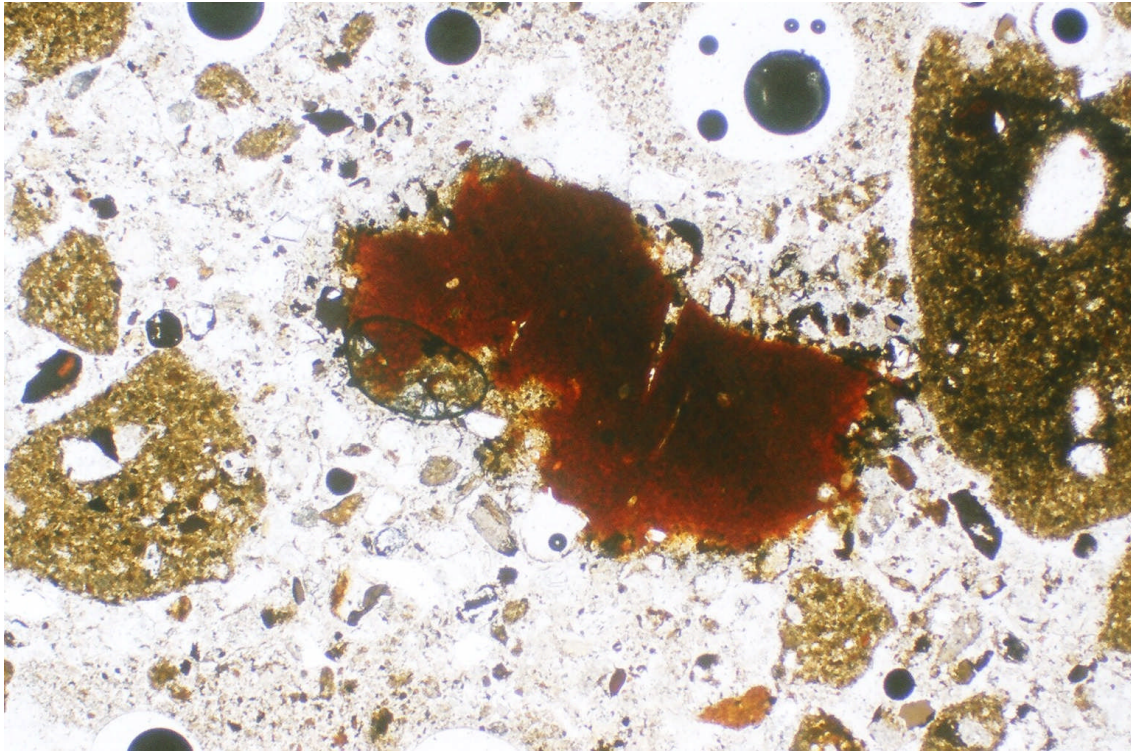


Figure 29. Sample 006 in plain transmitted light, width of field 2.6 mm, showing a large particle of reddish, heterogeneous Fe oxyhydroxide. The spectrum of the particle is similar to those obtained for Ca–Cu-rich particles in sample 004.